Fuzzy structure theory modeling of sound-insulation layers in complex vibroacoustic uncertain systems: Theory and experimental validation

C. Fernandez, Christian Soize, L. Gagliardini

Fuzzy structure theory modeling of sound-insulation layers in complex vibroacoustic uncertain sytems - Theory and experimental validation

Charles Fernandez and Christian Soize*

Universite Paris-Est,

Laboratoire Modelisation et Simulation Multiechelle FRE3160 CNRS,

5 bd Descartes,

77454 Marne-la-Vallee,

France

Laurent Gagliardini

PSA Peugeot-Citroen,

CTV,

route de Gisy,

78943 Velizy-Villacoublay Cedex France

(Dated: September 11, 2008)

Abstract

The fuzzy structure theory was introduced twenty years ago in order to model the effects of complex subsystems unprecisely known on a master structure. This theory was only aimed at structural dynamics. In this paper, an extension of that theory is proposed in developing an elastoacoustic element useful to model sound-insulation layers for computational vibroacoustics of complex systems. The simplified model constructed enhances computation time and memory allocation because the number of physical and generalized degrees of freedom in the computational vibroacoustic model is not increased. However, these simplifications introduce model uncertainties. In order to take into account these uncertainties, the nonparametric probabilistic approach recently introduced is used. A robust simplified model for sound-insulation layers is then obtained. This model is controlled by a small number of physical and dispersion parameters. Firstly, the extension of the fuzzy structure theory to elastoacoustic element is presented. Secondly, the computational vibroacoustic model including such an elastoacoustic element to model sound-insulation layer is given. Then, a design methodology to identify the model parameters with experiments is proposed and is experimentally validated. Finally, the theory is applied to an uncertain vibroacoustic system.

PACS numbers: 43.40At

I. INTRODUCTION

This paper deals with the construction of a robust model of sound-insulation layers required by computational vibroacoustics simulation of complex systems in low- and medium-frequency ranges. The sound-insulation layer is assumed to behave as a resonant continuous dynamical system in the frequency band of interest. In this paper, we will not consider the high frequency range where more elastic modes may appear. For such a modeling in the low- and medium-frequency ranges, a usual approach consists in modeling a sound-insulation layer as a poro-elastic medium using the Biot theory; the finite element method is then classically used to solve the associated boundary value problem. In this case, both vibroacoustic system and sound-insulation layers are modeled by the finite element method (see for instance Refs. [1–7]). When the first thickness eigenfrequencies belong to the frequency band of analysis, as assumed here, such a finite element model of sound-insulation layer introduces a large number of physical degrees of freedom (DOF) in the computational model as well as numerous elastic modes in the band. The size of the associated reduced computational model is then amply increased. For instance, in a car booming noise analysis (frequency range $[20, 200]$ Hz later referred as low frequency range), the finite element model may involve up to two millions of DOF for the structure and the reduced model requires about one thousand elastic modes. If the sound-insulation layers were modeled by the finite element method, an additional number of about five millions of DOF would be necessary. Twenty thousand additional elastic modes then appear in the reduced computational model exceeding the limits of current computational ressources. Consequently, there is a great interest to construct simplified sound-insulation layer models without adding neither physical DOF nor generalized DOF. Representing the sound-insulation layer by an adapted wall impedance can be a way to avoid the increase of DOF number (see for instance Refs. [8–12] for the notion of wall impedance in vibroacoustics). A great number of publications has been devoted to this subject in the last three decades. It should be noted that the largest part of

*Electronic address: christian.soize@univ-paris-est.fr

these works deals with the medium- and high-frequency ranges, where the sound-insulation layer behavior differs from the lower frequency range that is investigated here. Since the objective of this paper is not to give a state of the art on this particular topic, we simply refer to a few papers such as Refs. [13–23].

In this paper, an alternate construction to the finite element approach or to the usual wall impedances is presented. Firstly, this construction does not increase the number of physical and generalized DOF in the computational vibroacoustic model. Secondly, it does not involve the poroelastic equations because the sound-insulation layers considered here have a rather simple dynamic behavior which does not require advanced material modeling. As explained above, in the frequency band of analysis, the simplified model can be originated from a single DOF dynamical system. Due to the large variability of geometry, materials properties and connections to the master structure -mainly induced by the industrial process as well as vehicle diversity in the automotive industry for example-, the sound-insulation layer is considered as complex and therefore, a statistical description of its internal dynamical DOF is proposed. We are naturally leaded to use the fuzzy structure theory which fits this framework and has already been validated. A representation of the sound-insulation layer based on the fuzzy structure theory benefits from an understandable interpretation of complex dynamical systems behavior. It is simply characterized by a few physical parameters: the participating mass, the modal density and the internal damping rate. The fuzzy structure theory was introduced twenty years ago in order to model the effects on a master structure of complex subsystems imprecisely known (see Refs. [24–28]). This theory is developed in the context of the probability theory which is well adapted to this kind of problem that carries many uncertainties (geometry, material and boundary conditions). Many other works have been developed in this field, completing the initial construction (see Refs. [29–36]). Most of these developments are related to complex structural subsystems coupled to a master vibroacoustic system. No attempt has been performed to develop a specific sound-insulation layer model using the fuzzy structure theory. The known results have to be extended in order to build an elastoacoustic element. That is the aim of this pa-

per. However, such a simplified model introduces model uncertainties. In the original theory introduced in Ref. [24], the system parameters uncertainties were already taken into account with a parametric probabilistic approach. Today, it is well understood that the parametric probabilistic approach can only address system parameters uncertainties but not model uncertainties. Recently, a nonparametric probabilistic approach has been introduced (see Refs. [37–40]), allowing both system parameters uncertainties and model uncertainties to be taken into account in the computational model. The use of a nonparametric probabilistic approach to take into account model uncertainties in the sound-insulation layer simplified model constitutes a new extension of the fuzzy structure theory with respect to the model uncertainties problems. In addition, a complete design methodology is experimentally validated; this two-steps methodology can easily be implemented in the current engineering process of mechanical devices.

In order to help the understanding, we summarize below the modeling strategy used in this paper. As explained above, a complete three dimensional modeling of the sound-insulation layer would consist in introducing a poroelastic medium and such an approach would lead us to introduce a large additional number of DOF in the computational model. A way to construct a simplified model could have consisted in introducing an empirical simplified model for which the identification would have been equivalent to a "curve-fitting". Such a way is not used here. In opposite, the proposed simplified model is constructed using the fuzzy structure theory for which the main dynamical physical phenomena are captured and are taken into account. In the frequency band of interest, the major phenomena are due to the internal resonances of the sound-insulation layer. The fuzzy structure theory allows hidden dynamical DOF effects on the master structure to be taken into account in the sense of in statistical averaging. With such a theory, the power flow between the fuzzy subsystem (the sound-insulation layer) and the master vibroacoustic system is mainly controlled by the resonances of the sound-insulation layer, by the participating dynamical mass and by the internal damping. The corresponding parameters of the model are, as explained above, the mean modal density of the internal resonances, the coefficient of participating mass defined

with respect to the total physical mass and finally, the damping rate. It should be noted that the mean modal density which strongly depends on the geometry and on the materials is unknown but can be estimated with a usual computational model of the sound-insulation layer as proposed in this paper. Note that such computations are usually performed in industrial engineering processes. Such an estimation is then realistic for practical applications of complex systems. The total mass of the sound-insulation layer is known but the coefficient of participating mass is generally unknown for frequencies larger that the cut-off frequency (which is the known first eigenfrequency of the sound-insulation layer) and has to be identified, for instance using experiments. This coefficient is less sensitive to the geometry than the modal density. In engineering practice, when this coefficient has been identified for given materials and a given thickness, the identified value can be reused for similar sound-insulation layers without performing a new identification. Clearly, an error is introduced but this error is taken into account by the probabilistic model of uncertainties. So, as soon as a class of sound-insulation layers has been identified, the model can be used for any geometry because for each fixed geometry of a sound-insulation layer, its cut-off frequency and modal density are computed with a usual finite element model. This methodology shows that the proposed model of the sound-insulation layer does not correspond to the "curve-fitting" of an empirical model.

Section II is devoted to the construction of the sound-insulation layer simplified mean model using the fuzzy structure theory. As far as this model is part of a complex vibroacoustic system, the complete vibroacoustic model is presented. In this context, the nominal model will also be called the "mean model" and it refers to the deterministic model which does not take into account uncertainties. Section III deals with the finite element approximation which allows a computational vibroacoustic mean model to be constructed. In Section IV, we present the first step of the methodology performing the experimental identification of the mean parameters of the sound-insulation layer simplified model. Section V is devoted to the construction of the computational stochastic model for the uncertain vibroacoustic system including the uncertain sound-insulation layer. Some aspects relative to the stochatic

solver are also presented in this section. Section VI addresses the second step of the methodology where the experimental identification of the dispersion parameters of the probabilistic model is performed. The identification of the dispersion parameters relative to the structure is performed using an experimental database while a reference numerical solution is used to identify the dispersion parameters relative to the probabilistic model of the sound-insulation layer. Finally, Section VII deals with the prediction of the system's vibroacoustic response using the previously identified computational stochastic model.

II. CONSTRUCTION OF A SIMPLIFIED MEAN MODEL OF THE SOUND-INSULATION LAYER USING THE FUZZY STRUCTURE THEORY IN A VIBROACOUSTIC SYSTEM

A. Definition of the vibroacoustic system

The physical space $\mathbb{R}^3$ is referred to a cartesian system for which the generic point is denoted by $\boldsymbol{x} = (x_1, x_2, x_3)$. The Fourier transform with respect to time t is denoted by $u(\omega) = \int_{\mathbb{R}} e^{-i\omega t} u(t)\, dt$. The vibroacoustic system is analyzed in the frequency band $\mathbb{B} = [\omega_{min}, \omega_{max}]$. The structure occupies a three-dimensioned bounded domain Ω_s and is modeled by a nonhomogeneous anisotropic viscoelastic material. The boundary of Ω_s is written as $\partial\Omega_s = \Gamma_s \cup \Gamma_0 \cup \Gamma_1 \cup \Gamma_2$ (see Fig.1) and the outward unit normal to $\partial\Omega_s$ is $\boldsymbol{n}^s(\boldsymbol{x})$. The structure is fixed on Γ_0, a surface force field $\boldsymbol{g}^{surf}(\boldsymbol{x}, \omega)$ is given on Γ_1 and a body force field $\boldsymbol{g}^{vol}(\boldsymbol{x}, \omega)$ is given in Ω_s. The acoustic cavity Ω_a is filled with a dissipative acoustic fluid, its boundary is written as $\partial\Omega_a = \Gamma \cup \Gamma_2$ and the inward unit normal to $\partial\Omega_a$ is $\boldsymbol{n}(\boldsymbol{x})$ (note that $\boldsymbol{n}(\boldsymbol{x}) = \boldsymbol{n}^s(\boldsymbol{x})$ on Γ_2 and that without sound-insulation layer, the coupling surface $\partial\Omega_a$ between the structure and the cavity would be $\Gamma_s \cup \Gamma_2$). A sound-insulation layer which occupies a bounded domain Ω_h with boundary $\partial\Omega_h = \Gamma \cup \Gamma_s$ is attached to the part Γ_s of the boundary of the structure (see Fig.1). Let $\boldsymbol{x} \mapsto \boldsymbol{u}^s(\boldsymbol{x}, \omega) = (u_1^s(\boldsymbol{x}, \omega), u_2^s(\boldsymbol{x}, \omega), u_3^s(\boldsymbol{x}, \omega))$ be the structural displacement field defined on Ω_s with values in $\mathbb{C}^3$ and which is equal to zero on Γ_0. Let $\boldsymbol{x} \mapsto p(\boldsymbol{x}, \omega)$ be the pressure field inside Ω_a with value in $\mathbb{C}$ for which the value on

$\partial\Omega_a = \Gamma \cup \Gamma_2$ is still denoted by $p(\boldsymbol{x},\omega)$. Let $\boldsymbol{x} \mapsto \boldsymbol{u}^h(\boldsymbol{x},\omega) = (u_1^h(\boldsymbol{x},\omega), u_2^h(\boldsymbol{x},\omega), u_3^h(\boldsymbol{x},\omega))$ be the sound-insulation layer displacement field defined on Ω_h with values in $\mathbb{C}^3$ whose value on interface Γ is still denoted by $\boldsymbol{x} \mapsto \boldsymbol{u}^h(\boldsymbol{x},\omega)$. Finally, we need to introduce the admissible spaces for the three fields of the problem. Let $\mathcal{C}_0^s$ be the space of the admissible displacement fields of the structure such that $\boldsymbol{u}^s = 0$ on Γ_0, let $\mathcal{C}^a$ be the space of the admissible pressure fields in the acoustic cavity and $\mathcal{C}^h$ be the space of the admissible displacement fields of the sound-insulation layer.

B. Coupling force fields

The coupling force field on boundary Γ_s that the structure exerts on the sound-insulation layer is denoted by $\boldsymbol{x} \mapsto \boldsymbol{f}^s(\boldsymbol{x},\omega) = (f_1^s(\boldsymbol{x},\omega), f_2^s(\boldsymbol{x},\omega), f_3^s(\boldsymbol{x},\omega))$ and can be written for all $\boldsymbol{x}$ fixed in Γ_s as $\boldsymbol{f}^s(\boldsymbol{x},\omega) = f^s(\boldsymbol{x},\omega)\boldsymbol{n}^s(\boldsymbol{x}) + \boldsymbol{f}_{tang}^s(\boldsymbol{x},\omega)$. It is assumed that the tangential force field $\boldsymbol{f}_{tang}^s(\boldsymbol{x},\omega)$ exerted by the structure on the sound-insulation layer is equal to zero. This hypothesis is reasonable in vibroacoustics for the majority of the cases met in the technologies such as the ones used in the automotive industry. Nevertheless, this hypothesis is not perfectly satisfied for real complex systems and induces uncertainties in the vibroacoustic model. This is a reason why a model of uncertainties will be introduced. Consequently, we have

$$\boldsymbol{f}^s(\boldsymbol{x},\omega) = f^s(\boldsymbol{x},\omega)\boldsymbol{n}^s(\boldsymbol{x}) \quad . \tag{1}$$

Note that dimension of $f_i^s(\boldsymbol{x},t)$ is $[M][L]^{-1}[T]^{-2}$. The coupling force field $\boldsymbol{x} \mapsto \boldsymbol{f}^p(\boldsymbol{x},\omega) = (f_1^p(\boldsymbol{x},\omega), f_2^p(\boldsymbol{x},\omega), f_3^p(\boldsymbol{x},\omega))$ on boundary $\partial\Omega_a = \Gamma \cup \Gamma_2$ that the acoustic fluid exerts on the structure (interface Γ_2) and the sound-insulation layer (interface Γ) is written as,

$$\boldsymbol{f^p}(\boldsymbol{x},\omega)ds(\boldsymbol{x}) = -p(\boldsymbol{x},\omega)\boldsymbol{n}(\boldsymbol{x})ds(\boldsymbol{x}) \tag{2}$$

in which ds is the surface element on $\partial\Omega_a$. The equations of the boundary value problem for the vibroacoustic system made up of the structure coupled with internal acoustic cavity and with the sound-insulation layer are given in Appendix A. Eqs. (A4), (A5) and (A6) are the equations for the structure, the acoustic cavity and the sound-insulation layer. There

are coupling terms in these three equations. In particular, the coupling term between the sound-insulation layer and the structure in the Eq. (A4) of the structure is represented by the term $c_{\Gamma_s}(\boldsymbol{\delta u}^s;\omega)$; the coupling term between the sound-insulation layer and the acoustic cavity in Eq. (A5) of the acoustic cavity is represented by the term $c_{\Gamma}(\boldsymbol{u}^h,\delta p)$. The principle of construction of the simplified model for the sound-insulation layer consists in replacing Eq. (A6) by a simplified model obtained in using the fuzzy structure theory[24,26,27] for which a synthesis is given in Ref [12]. This means that the two coupling terms $c_{\Gamma_s}(\boldsymbol{\delta u}^s;\omega)$ and $c_{\Gamma}(\boldsymbol{u}^h,\delta p)$ have to be expressed as a function of $\boldsymbol{u}^s$ and p using the fuzzy structure theory. This theory consists (1) in introducing an underlying deterministic dynamical model (see Section II.C), (2) in introducing a probabilistic model of the eigenfrequencies of this dynamical model (see Section II.D) and (3) in performing a statistical averaging (see Section II.E).

C. Definition of the underlying deterministic model for the fuzzy structure

We introduce the following hypothesis for the sound-insulation layer (see Fig. 2): the surfaces Γ and Γ_s are assumed to be geometrically equivalent and consequently, for all $\boldsymbol{x}$ in $\Gamma_s \simeq \Gamma$, $\boldsymbol{n}^s(\boldsymbol{x}) \simeq \boldsymbol{n}(\boldsymbol{x})$. The normal component to Γ_s of the structural displacement field is

$$\boldsymbol{n}^s(\boldsymbol{x}).\boldsymbol{u}^s(\boldsymbol{x},\omega) = w^s(\boldsymbol{x},\omega) \quad , \quad \boldsymbol{x} \in \Gamma_s \quad . \tag{3}$$

The normal component to Γ of the displacement field of the sound-insulation layer is

$$\boldsymbol{n}(\boldsymbol{x}).\boldsymbol{u}^h(\boldsymbol{x},\omega) = w(\boldsymbol{x},\omega) \tag{4}$$

in which $\boldsymbol{n}(\boldsymbol{x}) \simeq \boldsymbol{n}^s(\boldsymbol{x})$, for $\boldsymbol{x} \in \Gamma_s \simeq \Gamma$. Using the first step of the fuzzy structure theory and taking into account the hypothesis introduced in Section II.B, the underlying deterministic model is made up of a density of damped linear oscillators acting in the normal direction to Γ. For a fixed frequency ω and for a fixed $\boldsymbol{x}$ in Γ_s, the displacement of the base of an oscillator is $w^s(\boldsymbol{x},\omega)$ and the displacement of its mass $\mu(\boldsymbol{x},\omega) > 0$ is $w(\boldsymbol{x},\omega)$. The mass density $\mu(\boldsymbol{x},\omega)$ ($[M][L]^{-2}$) is distributed on Γ. The corresponding stiffness density

$k(\boldsymbol{x},\omega)$ associated with this oscillator is $k(\boldsymbol{x},\omega)=\mu(\boldsymbol{x},\omega)\omega_p^2(\boldsymbol{x},\omega)$ where $\omega_p(\boldsymbol{x},\omega)>0$ is the eigenfrequency (rad.s^{-1}) of the undamped linear oscillator with fixed base. The damping rate of this oscillator is denoted by $\xi(\boldsymbol{x},\omega)$. Let $\boldsymbol{f}^s(\boldsymbol{x},\omega)$ be the force applied to the base of this oscillator and corresponding to the force density induced by the structure on the sound-insulation layer (see Eq. (1)). Let $\boldsymbol{f}^p(\boldsymbol{x},\omega)$ be the force applied to the mass of the oscillator and corresponding to the force density induced by the acoustic pressure $p(\boldsymbol{x},\omega)$ on the sound-insulation layer (see Eq. (2)). Removing $\boldsymbol{x}$ and ω for brevity, the equation of this oscillator is written as

$$\mu \begin{bmatrix} -\omega^2+2i\omega\xi\omega_p+\omega_p^2 & -2i\omega\xi\omega_p-\omega_p^2 \\ -2i\omega\xi\omega_p-\omega_p^2 & 2i\omega\xi\omega_p+\omega_p^2 \end{bmatrix} \times \begin{bmatrix} w(\boldsymbol{x},\omega) \\ w^s(\boldsymbol{x},\omega) \end{bmatrix} = \begin{bmatrix} -p(\boldsymbol{x},\omega) \\ f^s(\boldsymbol{x},\omega) \end{bmatrix} . \quad (5)$$

For all ω in $\mathbb{B}$, from Eq. (5), it can be deduced that

$$w(\boldsymbol{x},\omega)=a^c(\boldsymbol{x},\omega)w^s(\boldsymbol{x},\omega)+\frac{1}{\omega^2}a^a(\boldsymbol{x},\omega)p(\boldsymbol{x},\omega)\ , \quad (6)$$

$$f^s(\boldsymbol{x},\omega)=a^s(\boldsymbol{x},\omega)w^s(\boldsymbol{x},\omega)+a^c(\boldsymbol{x},\omega)p(\boldsymbol{x},\omega) \quad (7)$$

in which

$$a^s(\boldsymbol{x},\omega)= \frac{-\omega^2\,\mu(\boldsymbol{x},\omega)\,(2i\omega\,\xi(\boldsymbol{x},\omega)\omega_p(\boldsymbol{x},\omega)+\omega_p(\boldsymbol{x},\omega)^2)}{-\omega^2+2i\omega\,\xi(\boldsymbol{x},\omega)\omega_p(\boldsymbol{x},\omega)+\omega_p(\boldsymbol{x},\omega)^2}\,, \quad (8)$$

$$a^a(\boldsymbol{x},\omega)= \frac{-\omega^2/\mu(\boldsymbol{x},\omega)}{-\omega^2+2i\omega\,\xi(\boldsymbol{x},\omega)\omega_p(\boldsymbol{x},\omega)+\omega_p(\boldsymbol{x},\omega)^2}\,, \quad (9)$$

$$a^c(\boldsymbol{x},\omega)= \frac{2i\omega\,\xi(\boldsymbol{x},\omega)\omega_p(\boldsymbol{x},\omega)+\omega_p(\boldsymbol{x},\omega)^2}{-\omega^2+2i\omega\,\xi(\boldsymbol{x},\omega)\omega_p(\boldsymbol{x},\omega)+\omega_p(\boldsymbol{x},\omega)^2}\,. \quad (10)$$

As explained in Section II.B, we have to express the two terms $c_{\Gamma}(\boldsymbol{u}^h, \delta p)$ and $c_{\Gamma_s}(\boldsymbol{\delta u}; \omega)$. Using $\Gamma \simeq \Gamma_s$, substituting Eq. (4) into $c_{\Gamma}(\boldsymbol{u}^h, \delta p)$ defined by Eq. (A2), substituting Eq. (6) again into Eq. (A2) and using Eq. (3) yield

$$\begin{aligned} & \omega^2 c_{\Gamma}(\boldsymbol{u}^h, \delta p) \\ = & \omega^2 \int_{\Gamma_s} a^c(\boldsymbol{x}, \omega)\, \boldsymbol{n}^s(\boldsymbol{x}).\boldsymbol{u}^s(\boldsymbol{x}, \omega)\, \delta p(\boldsymbol{x})\, ds(\boldsymbol{x}) \\ & + \int_{\Gamma_s} a^a(\boldsymbol{x}, \omega)\, p(\boldsymbol{x}, \omega)\, \delta p(\boldsymbol{x})\, ds(\boldsymbol{x}) \quad . \end{aligned} \tag{11}$$

Substituting Eq. (1) into $c_{\Gamma_s}(\boldsymbol{\delta u}; \omega; \omega)$ defined by Eq. (A3), substituting Eq. (7) again into Eq. (A3) and using Eq. (3) yield

$$\begin{aligned} & c_{\Gamma_s}(\boldsymbol{\delta u}^s; \omega) \\ = & \int_{\Gamma_s} a^s(\boldsymbol{x}, \omega)\, (\boldsymbol{n}^s(\boldsymbol{x}).\boldsymbol{u}^s(\boldsymbol{x}, \omega))(\boldsymbol{n}^s(\boldsymbol{x}).\boldsymbol{\delta u}^s(\boldsymbol{x}))ds(\boldsymbol{x}) \\ & + \int_{\Gamma_s} a^c(\boldsymbol{x}, \omega) p(\boldsymbol{x}, \omega)\, (\boldsymbol{n}^s(\boldsymbol{x}).\boldsymbol{\delta u}^s(\boldsymbol{x}))\; ds(\boldsymbol{x})\,. \end{aligned} \tag{12}$$

D. Probabilistic model of the eigenfrequency of the oscillators

The second step of the fuzzy structure consists in modeling $\omega_p(\boldsymbol{x}, \omega)$ by a random variable $\Omega_p(\boldsymbol{x}, \omega)$. In this section, we then introduce the random bilinear form associated with $c_{\Gamma}(\boldsymbol{u}^h, \delta p)$ and the random linear form associated with $c_{\Gamma_s}(\boldsymbol{\delta u}^s; \omega)$ defined by Eqs. (11) and (12). For all ω in $\mathbb{B}$, we choose to represent $\mu(\boldsymbol{x}, \omega)$ and $\xi(\boldsymbol{x}, \omega)$ by their mean values $\mu(\boldsymbol{x}, \omega) = \underline{\mu}(\omega) > 0$ and $\xi(\boldsymbol{x}, \omega) = \underline{\xi}(\omega)$ where $\omega \mapsto \underline{\mu}(\omega)$ and $\omega \mapsto \underline{\xi}(\omega)$ are two deterministic functions independent of $\boldsymbol{x}$ with $0 < \underline{\xi}(\omega) < 1$. The mean participating mass can be written[24,26,27] as $\underline{\mu}(\omega) = \underline{\nu}(\omega) m_{\text{tot}}/|\Gamma_s|$ where $0 \leq \underline{\nu}(\omega) \leq 1$ is the mean coefficient of participating mass, m_{tot} is the total mass of the density of oscillators and $|\Gamma_s|$ is the measure of surface Γ_s. It should be noted that if there are several sound-insulation layers with different values of parameters $\underline{\mu}$ and $\underline{\xi}$, domain Ω_h is subdivised into several subdomains and thus, their parameters have to be constant with respect to $\boldsymbol{x}$ in every subdomain. For all $\boldsymbol{x}$ fixed in Γ_s and ω fixed in $\mathbb{B}$, the eigenfrequency $\omega_p(\boldsymbol{x}, \omega)$ is modeled by a positive

random variable $\Omega_p(\boldsymbol{x},\omega)$ whose probability distribution $P_{\Omega_p(\boldsymbol{x};\omega)}(d\omega_p,\omega)$ is assumed to be independent of $\boldsymbol{x}$ and is defined by the probability density function $p_{\Omega_p(\boldsymbol{x};\omega)}(\omega_p,\omega)$ with respect to $d\omega_p$, such that[24,26]

$$p_{\Omega_p(\boldsymbol{x};\omega)}(\omega_p,\omega) = \ell(\omega)\mathbb{1}_{[a(\omega),b(\omega)]}(\omega_p) \quad , \tag{13}$$

with $\mathbb{1}_B(\boldsymbol{x}) = 1$ if $\boldsymbol{x} \in B$ and $= 0$ if $\boldsymbol{x} \notin B$ and where

$$a(\omega) = \sup\left\{0, \omega - \frac{1}{2\underline{n}(\omega)}\right\} \quad , \tag{14}$$

$$b(\omega) = \omega + \frac{1}{2\underline{n}(\omega)} \quad , \tag{15}$$

$$\ell(\omega) = \frac{1}{b(\omega) - a(\omega)} \tag{16}$$

in which $\underline{n}(\omega)$ is the mean modal density of the sound-insulation layer. In order to better explain the meaning of parameters $\underline{n}(\omega)$ and $\underline{\mu}(\omega)$, we define them in the simplest case for which the fuzzy structure Ω_h would be made up of $N_{\rm osc}$ oscillators uniformly distributed in the frequency band $\mathbb{B}$ and uniformly distributed on surface Γ_s. In this case, the mass of each oscillator would be $m_{\rm osc}$. Consequently, the total mass of the fuzzy structure would be $m_{\rm tot} = N_{\rm osc} m_{\rm osc}$ and for all $\boldsymbol{x}$ in Γ_s, we would have $\mu(\boldsymbol{x},\omega) = \underline{\mu}(\omega) = \sqrt{N_{\rm osc}} m_{\rm osc}/|\Gamma_s|$, $\int_{\mathbb{B}} \underline{n}(\omega) d\omega = \sqrt{N_{\rm osc}}$ and $\int_{\mathbb{B}} \underline{\mu}(\omega)\underline{n}(\omega) d\omega = m_{\rm tot}/|\Gamma_s|$. Coming back to the general case, for all $\boldsymbol{x}$ fixed in Γ_s and ω fixed in $\mathbb{B}$, the coefficients $a^s(\boldsymbol{x},\omega)$, $a^a(\boldsymbol{x},\omega)$ and $a^c(\boldsymbol{x},\omega)$ defined by Eqs. (8), (9) and (10) become random variables denoted by $A^s(\boldsymbol{x},\omega)$, $A^a(\boldsymbol{x},\omega)$ and $A^c(\boldsymbol{x},\omega)$. For all $\boldsymbol{u}^s$ and $\boldsymbol{\delta u}^s$ in $\mathcal{C}_0^s$ and for all p and δp in $\mathcal{C}^a$, the forms $c_{\Gamma}(\boldsymbol{u}^h, \delta p)$ and $c_{\Gamma_s}(\boldsymbol{\delta u}^s;\omega)$ defined by Eqs. (11) and (12) become random variables which are rewritten in terms of $\boldsymbol{u}^s, p, \boldsymbol{\delta u}^s$ and δp as $C_{\Gamma}(\boldsymbol{u}^s, p, \delta p;\omega)$ and $C_{\Gamma_s}(\boldsymbol{u}^s, p, \boldsymbol{\delta u}^s;\omega)$ and which are such that

$$\begin{aligned} &\omega^2 C_{\Gamma}(\boldsymbol{u}^s, p, \delta p;\omega) \\ &= \omega^2 \int_{\Gamma_s} A^c(\boldsymbol{x},\omega)\, \boldsymbol{n}^s(\boldsymbol{x}).\boldsymbol{u}^s(\boldsymbol{x},\omega)\, \delta p(\boldsymbol{x})\, ds(\boldsymbol{x}) \\ &+ \int_{\Gamma_s} A^a(\boldsymbol{x},\omega)\, p(\boldsymbol{x},\omega)\, \delta p(\boldsymbol{x})\, ds(\boldsymbol{x}) \end{aligned} \tag{17}$$

and

$$
\begin{aligned}
& C_{\Gamma_s}(\boldsymbol{u}^s, p, \boldsymbol{\delta u}^s; \omega) \\
&= \int_{\Gamma_s} A^s(\boldsymbol{x}, \omega)\ (\boldsymbol{n}^s(\boldsymbol{x}).\boldsymbol{u}^s(\boldsymbol{x}, \omega))\, (\boldsymbol{n}^s(\boldsymbol{x}).\boldsymbol{\delta u}^s(\boldsymbol{x}))\ ds(\boldsymbol{x}) \\
&+ \int_{\Gamma_s} A^c(\boldsymbol{x}, \omega) p(\boldsymbol{x}, \omega)\, (\boldsymbol{n}^s(\boldsymbol{x}).\boldsymbol{\delta u}^s(\boldsymbol{x}))\ ds(\boldsymbol{x}) \quad . \qquad (18)
\end{aligned}
$$

E. Statistical averaging and simplified mean model of the sound-insulation layer

The last step of the fuzzy structure theory consists in defining the simplified mean model taking the statistical averaging of random variables $C_\Gamma(\boldsymbol{u}^s, p, \delta p; \omega)$ and $C_{\Gamma_s}(\boldsymbol{u}^s, p, \boldsymbol{\delta u}^s; \omega)$ defined by Eqs. (17) and (18). As we have explained in section II.B, the simplified mean model thus consists in replacing the two coupling terms $c_\Gamma(\boldsymbol{u}^h, \delta p)$ and $c_{\Gamma_s}(\boldsymbol{\delta u}^s; \omega)$ by $\underline{c}_\Gamma(\boldsymbol{u}^s, p, \delta p; \omega)$ and $\underline{c}_{\Gamma_s}(\boldsymbol{u}^s, p, \boldsymbol{\delta u}^s; \omega)$ such that,

$$
\underline{c}_\Gamma(\boldsymbol{u}^s, p, \delta p; \omega) = \mathcal{E}\{C_\Gamma(\boldsymbol{u}^s, p, \delta p; \omega)\} \quad , \qquad (19)
$$

$$
\underline{c}_{\Gamma_s}(\boldsymbol{u}^s, p, \boldsymbol{\delta u}^s; \omega) = \mathcal{E}\left\{C_{\Gamma_s}(\boldsymbol{u}^s, p, \boldsymbol{\delta u}^s; \omega)\right\} \qquad (20)
$$

in which $\mathcal{E}$ is the mathematical expectation. Analyzing Eqs. (17) and (18) leads us to introduce the following deterministic bilinear forms $b^s(\boldsymbol{u}^s, \boldsymbol{\delta u}^s)$ on $\mathcal{C}_0^s \times \mathcal{C}_0^s$, $c^s(p, \boldsymbol{\delta u}^s)$ on $\mathcal{C}^a \times \mathcal{C}_0^s$ and $b^a(p, \delta p)$ on $\mathcal{C}^a \times \mathcal{C}^a$,

$$
b^s(\boldsymbol{u}^s, \boldsymbol{\delta u}^s) = \int_{\Gamma_s} (\boldsymbol{n}^s(\boldsymbol{x}).\boldsymbol{u}^s(\boldsymbol{x}))\, (\boldsymbol{n}^s(\boldsymbol{x}).\boldsymbol{\delta u}^s(\boldsymbol{x}))\ ds(\boldsymbol{x})\,, \qquad (21)
$$

$$
c^s(p, \boldsymbol{\delta u}^s) = \int_{\Gamma_s} p(\boldsymbol{x})\, (\boldsymbol{n}^s(\boldsymbol{x}).\boldsymbol{\delta u}^s(\boldsymbol{x}))\ ds(\boldsymbol{x}) \quad , \qquad (22)
$$

$$
b^a(p, \delta p) = \int_{\Gamma_s} p(\boldsymbol{x})\, \delta p(\boldsymbol{x})\, ds(\boldsymbol{x}) \quad . \qquad (23)
$$

From Eqs. (17) and (18) and using Eqs. (19) and (20) with Eqs. (13) to (16) yield

$$
\omega^2 \underline{c}_\Gamma(\boldsymbol{u}^s, p, \delta p; \omega) = \omega^2 \underline{a}^c(\omega)\, c^s(\delta p, \boldsymbol{u}^s) + \underline{a}^a(\omega)\, b^a(p, \delta p)\,, \qquad (24)
$$

$$
\underline{c}_{\Gamma_s}(\boldsymbol{u}^s, p, \boldsymbol{\delta u}^s; \omega) = \underline{a}^s(\omega)\, b^s(\boldsymbol{u}^s, \boldsymbol{\delta u}^s) + \underline{a}^c(\omega)\, c^s(p, \boldsymbol{\delta u}^s) \qquad (25)
$$

in which

$$\underline{a}^s(\omega) = -\omega^2 \underline{a}^s_R(\omega) + i\omega \underline{a}^s_I(\omega) \quad , \tag{26}$$

$$\underline{a}^a(\omega) = \underline{a}^a_R(\omega) + i\omega \underline{a}^a_I(\omega), \tag{27}$$

$$\underline{a}^c(\omega) = \underline{a}^c_R(\omega) + i\underline{a}^c_I(\omega) \quad , \tag{28}$$

with

$$\underline{a}^s_R(\omega) = \underline{\mu}(\omega)\underline{n}(\omega) \ \left[\frac{1}{\underline{n}(\omega)} - \omega\, \underline{\lambda}(\omega)\, \Theta_{_R}(\omega)\right], \tag{29}$$

$$\underline{a}^s_I(\omega) = \underline{\mu}(\omega)\underline{n}(\omega)\ \omega^2 \underline{\lambda}(\omega)\ \Theta_{_I}(\omega)\,, \tag{30}$$

$$\underline{a}^a_R(\omega) = \omega\, \underline{n}(\omega)\ \frac{\underline{\lambda}(\omega)}{\underline{\mu}(\omega)}\ \Theta_{_R}(\omega) \quad , \tag{31}$$

$$\underline{a}^a_I(\omega) = \underline{n}(\omega)\ \frac{\underline{\lambda}(\omega)}{\underline{\mu}(\omega)}\ \Theta_{_I}(\omega) \quad , \tag{32}$$

$$\underline{a}^c_R(\omega) = 1 - \omega\, \underline{n}(\omega)\underline{\lambda}(\omega)\ \Theta_{_R}(\omega) \quad , \tag{33}$$

$$\underline{a}^c_I(\omega) = -\omega\, \underline{n}(\omega)\underline{\lambda}(\omega)\ \Theta_{_I}(\omega) \quad . \tag{34}$$

In these equations, the functions $\underline{\lambda}$, $\Theta_{_R}$ and $\Theta_{_I}$ are defined in Appendix B. We then deduce the simplified mean model of the sound-insulation layer: Find $\boldsymbol{u}^s$ in $\mathcal{C}^s_0$ and p in $\mathcal{C}^a$ such that, for all $\boldsymbol{\delta u}^s$ in $\mathcal{C}^s_0$ and δp in $\mathcal{C}^a$, we have

$$\begin{aligned}
&-\omega^2 m^s(\boldsymbol{u}^s, \boldsymbol{\delta u}^s) + i\omega\, d^s(\boldsymbol{u}^s, \boldsymbol{\delta u}^s; \omega) \\
&+ k^s(\boldsymbol{u}^s, \boldsymbol{\delta u}^s; \omega) + c_{_{\Gamma_2}}(\boldsymbol{\delta u}^s, p) \\
&+ \underline{a}^s(\omega) b^s(\boldsymbol{u}^s, \boldsymbol{\delta u}^s) + \underline{a}^c(\omega) c^s(p, \boldsymbol{\delta u}^s) = l^s(\boldsymbol{\delta u}^s; \omega)\,,
\end{aligned} \tag{35}$$

$$\begin{aligned}
&-\omega^2 m^a(p, \delta p) + i\omega\, d^a(p, \delta p; \omega) + k^a(p, \delta p) \\
&+ \omega^2 c_{_{\Gamma_2}}(\boldsymbol{u}^s, \delta p) + \omega^2 \underline{a}^c(\omega) c^s(\delta p, \boldsymbol{u}^s) \\
&+ \underline{a}^a(\omega) b^a(p, \delta p) = l^a(\delta p; \omega)
\end{aligned} \tag{36}$$

in which the bilinear forms b^s, c^s and b^a are defined by Eqs. (21), (22) and (23) and where m^s, d^s, k^s, m^a, d^a, k^a and $c_{_{\Gamma_2}}$ are defined by Eqs. (A7) to (A13).

III. COMPUTATIONAL VIBROACOUSTIC MEAN MODEL

The finite element discretization[12,44] of Eqs. (35) and (36) yields the following matrix equation on $\mathbb{C}^{m_s} \times \mathbb{C}^{m_a}$ defined by Eqs. (17) and (18),

$$\begin{bmatrix} [\underline{\mathbb{A}}^s(\omega)] + \underline{a}^s(\omega)[\underline{\mathbb{B}}^s] & [\underline{\mathbb{C}}] + \underline{a}^c(\omega)[\underline{\mathbb{C}}^s] \\ \omega^2\big\{[\underline{\mathbb{C}}]^T + \underline{a}^c(\omega)[\underline{\mathbb{C}}^s]^T\big\} & [\underline{\mathbb{A}}^a(\omega)] + \underline{a}^a(\omega)[\underline{\mathbb{B}}^a] \end{bmatrix} \times \begin{bmatrix} \underline{\boldsymbol{u}}^s(\omega) \\ \underline{\boldsymbol{p}}(\omega) \end{bmatrix} = \begin{bmatrix} \underline{\mathbb{f}}^s(\omega) \\ \underline{\mathbb{f}}^a(\omega) \end{bmatrix} \quad , \tag{37}$$

where $[\underline{\mathbb{A}}^s(\omega)]$ is a complex $(m_s \times m_s)$ matrix such that

$$[\underline{\mathbb{A}}^s(\omega)] = -\omega^2\,[\underline{\mathbb{M}}^s] + i\omega\,[\underline{\mathbb{D}}^s(\omega)] + [\underline{\mathbb{K}}^s(\omega)] \tag{38}$$

in which $[\underline{\mathbb{M}}^s]$, $[\underline{\mathbb{D}}^s(\omega)]$ and $[\underline{\mathbb{K}}^s(\omega)]$ are the mass, damping and stiffness matrices of the structure *in vacuo*. In Eq. (37), $[\underline{\mathbb{A}}^a(\omega)]$ is a complex $(m_a \times m_a)$ matrix,

$$[\underline{\mathbb{A}}^a(\omega)] = -\omega^2\,[\underline{\mathbb{M}}^a] + i\omega\,[\underline{\mathbb{D}}^a(\omega)] + [\underline{\mathbb{K}}^a] \tag{39}$$

in which $[\underline{\mathbb{M}}^a]$, $[\underline{\mathbb{D}}^a(\omega)]$ and $[\underline{\mathbb{K}}^a]$ are the "mass", "damping" and "stiffness" matrices of the acoustic cavity with rigid wall. The real $(m_s \times m_a)$ matrix $[\underline{\mathbb{C}}]$ is the usual vibroacoustic coupling matrix relative to boundary Γ_2 (which is without sound-insulation layer). The matrices $[\underline{\mathbb{B}}^s]$, $[\underline{\mathbb{C}}^s]$ and $[\underline{\mathbb{B}}^a]$ correspond to the finite element approximation of the bilinear forms defined by Eqs. (21), (22) and (23) respectively. Using n_s structural elastic modes *in vacuo* and n_a acoustic modes of the cavity with rigid walls including the constant pressure mode, the mean reduced matrix model of the vibroacoustic system is written as

$$\underline{\boldsymbol{u}}^s(\omega) = [\underline{\Phi}^s]\underline{\boldsymbol{q}}^s(\omega) \quad , \quad \underline{\boldsymbol{p}}(\omega) = [\underline{\Phi}^a]\underline{\boldsymbol{q}}^a(\omega) \quad , \tag{40}$$

$$\begin{bmatrix} [\underline{A}^s(\omega)] + \underline{a}^s(\omega)[\underline{B}^s] & [\underline{C}] + \underline{a}^c(\omega)[\underline{C}^s] \\ \omega^2\big\{[\underline{C}]^T + \underline{a}^c(\omega)[\underline{C}^s]^T\big\} & [\underline{A}^a(\omega)] + \underline{a}^a(\omega)[\underline{B}^a] \end{bmatrix} \times \begin{bmatrix} \underline{\boldsymbol{q}}^s(\omega) \\ \underline{\boldsymbol{q}}^a(\omega) \end{bmatrix} = \begin{bmatrix} \underline{\boldsymbol{f}}^s(\omega) \\ \underline{\boldsymbol{f}}^a(\omega) \end{bmatrix} \tag{41}$$

in which $[\underline{\Phi}^s]$ is the $(m_s \times n_s)$ real matrix of the structural modes, $[\underline{\Phi}^a]$ is the $(m_a \times n_a)$ real matrix of the acoustic modes, $[\underline{C}]$ is the $(n_s \times n_a)$ generalized vibroacoustic coupling matrix, $\underline{a}^s(\omega)[\underline{B}^s]$ is the $(n_s \times n_s)$ generalized matrix, $\underline{a}^c(\omega)[\underline{C}^s]$ is the $(n_s \times n_a)$ generalized matrix and $\underline{a}^a(\omega)[\underline{B}^a]$ is the $(n_a \times n_a)$ generalized matrix corresponding to the vibroacoustic coupling induced by the sound-insulation layer. The $(n_s \times n_s)$ matrix $[\underline{A}^s(\omega)]$ and the $(n_a \times n_a)$ matrix $[\underline{A}^a(\omega)]$ are written as

$$[\underline{A}^s(\omega)] = -\omega^2 [\underline{M}^s] + i\omega [\underline{D}^s(\omega)] + [\underline{K}^s(\omega)] \quad , \tag{42}$$

$$[\underline{A}^a(\omega)] = -\omega^2 [\underline{M}^a] + i\omega [\underline{D}^a(\omega)] + [\underline{K}^a] \tag{43}$$

in which $[\underline{M}^s]$, $[\underline{D}^s(\omega)]$ and $[\underline{K}^s(\omega)]$ are the generalized mass, damping and stiffness matrices of the structure and $[\underline{M}^a]$, $[\underline{D}^a(\omega)]$ and $[\underline{K}^a]$ are the generalized "mass", "damping" and "stiffness" matrices of the acoustic cavity.

IV. EXPERIMENTAL IDENTIFICATION OF THE MEAN PARAMETERS OF THE FUZZY STRUCTURE MODEL FOR THE SOUND-INSULATION LAYER - DESIGN METHODOLOGY PART 1

We propose to validate the simplified mean model of the sound-insulation layer by using experiments. The methodology used is the following:

(1) We consider a structure for which the experimental frequency response functions (FRF) are measured on frequency band $\mathbb{B}$.

(2) A sound-insulation layer is laid on this structure and the experimental FRF are measured again for the structure coupled with the sound-insulation layer.

(3) A mean computational model of the structure is developed and the model is updated using the experimental FRF measured in point (1) above.

(4) A mean computational model of the structure coupled with the sound-insulation layer is developed using the updated mean computational model of the structure and the simplified mean model of the sound-insulation layer. This simplified model provided by the fuzzy structure theory depends on unknown parameters $\underline{\xi}(\omega)$, $\underline{n}(\omega)$ and $\underline{\nu}(\omega)$ that we

propose to identify using the experimental FRF measured in point (2) above. The following methodology is carried out:

(4.i) Over all the frequency band $\mathbb{B}$, the mean damping rate $\underline{\xi}$ of the fuzzy part is assumed to be independent of ω and is fixed to its estimated value corresponding to the damping rate at the first experimental eigenfrequency.

(4.ii) The mean modal density $\underline{n}(\omega)$ is obtained by performing a modal analysis with a very fine mesh finite element model of the sound-insulation layer embedded on its base. We then calculate the mean number $\underline{N}(\omega)$ of eigenfrequencies in the frequency band $[0, \omega]$ and then, by a numerical derivative, we deduce the mean modal density $\underline{n}(\omega)$ which is such that $\underline{N}(\omega) = \int_0^\omega \underline{n}(\alpha) d\alpha$. The first eigenfrequency for which the mean modal density is different from zero is defined as the cut-off frequency Ω_C. This cut-off frequency can be viewed as the frequency for which the sound-insulation layer begins to act as a power flow transmitter due to its own thickness resonances (the internal dynamical resonances taken into account by the fuzzy structure theory).

(4.iii) For $\omega < \Omega_C$, the coefficient of participating mass $\underline{\nu}(\omega)$ is equal to 1 and the mean modal density $\underline{n}(\omega)$ is equal to 0. The three coefficients $\underline{a}^s(\omega)$, $\underline{a}^a(\omega)$ and $\underline{a}^c(\omega)$ (defined by Eqs (26), (27), (28)) are then taken as $\underline{a}^s(\omega) = -\underline{\mu}(\omega)\omega^2$, $\underline{a}^a(\omega) = 0$ and $\underline{a}^c(\omega) = 1$.

(4.iv) For $\omega \geq \Omega_C$, the parameter $\nu(\omega)$ is either experimentally identified by solving an inverse problem which is formulated as an optimization problem or is taken from a previous identified database.

A. Experimental configuration and measurements

The experimental configuration is made up of a homogeneous, isotropic and slightly damped thin plate (steel plate with a constant thickness) connected to an elastic framework on its edges. This structure is set horizontally and is hung up by four soft springs in order to avoid rigid body modes. The highest eigenfrequency of suspension is 9 Hz while the

lowest elastic mode of the structure is 43 Hz. The excitation is a point force applied to the framework and excites the dynamical system mainly in bending mode in the frequency band of analysis $\mathbb{B} =]0, 300]$ Hz. The number of sampling frequencies is $n_{\text{freq}} = 300$. The frequency resolution is $\Delta f = 1$ Hz. Sixty frequency response functions are performed for this structure. The frequency response functions $\omega \mapsto \gamma_i^{\text{exp}}(\omega)$ are identified on frequency band $\mathbb{B}$ for $n_{\text{obs}} = 60$ normal accelerations in the plate measured with a laser velocimeter. We then construct the following experimental frequency response function (FRF), $\omega \mapsto r^{\text{exp}}(\omega) = 10 \log_{10} (\sum_{i=1}^{n_{\text{obs}}} |\gamma_i^{\text{exp}}(\omega)|^2)$. This FRF has been chosen because it gives a robust and simple way to obtain the dynamical behavior of all the structure.

B. Experimental updating of the mean model of the structure without sound-insulation layer

The mean computational model of the structure is made up of a finite element model having $m_s = 57,768$ structural DOF. The reduced mean computational model is constructed with $n_s = 240$ structural modes. The mean computational model has been updated with respect to the Young modulus, the mass density and the damping rate of the plate and of the elastic framework using the experimental response of the system. The updated mean computational model will simply be called below the mean computational model. We introduce the function $\omega \mapsto r(\omega) = 10 \log_{10} (\sum_{i=1}^{n_{\text{obs}}} |\gamma_i(\omega)|^2)$. Figure 3 shows the comparison between the experimental measurements and the updated FRF of the mean computational model for the structure without the sound-insulation layer. We made the choice to update the mean computational model as follows. The level of the FRF has been updated at its experimental value of 29.9 dB at the first eigenfrequency. However, after such an updating, the first eigenfrequency given by the model stays at 42 Hz while the experimental value is at 43 Hz. We have also updated the first torsion eigenfrequency which is at 178 Hz (due to the framework) and nevertheless, the FRF level at this frequency is 37 dB while the experimental value is 42 dB. This strategy of updating has been chosen because the first elastic mode

and the torsion of the structure lightly depend on the sound-insulation layer. The other eigenfrequencies and the corresponding amplitudes of the responses have not specifically been updated. This is a source of uncertainties which is addressed below.

C. Experimental Identification of the parameters of the simplified model of the sound-insulation layer using a design methodology

A similar experimentation to the experiments described in section IV.B has been carried out when the structure is coupled with the sound-insulation layer which is made up of a heterogeneous, anisotropic, poroelastic foam and of a heavily damped septum (EPDM). The sound-insulation layer is laid on the plate and is not connected to the elastic framework. The reduced mean computational model is written (see Eq. (41)) as $[\underline{A}^s(\omega) + \underline{a}^s(\omega)[\underline{B}^s]]\,\underline{\boldsymbol{q}}^s(\omega) = \underline{\boldsymbol{f}}^s(\omega)$. We use this reduced mean computational model to identify the three parameters $\underline{\xi}$, $\underline{n}(\omega)$ and $\underline{\nu}(\omega)$ of the simplified model of the sound-insulation layer for ω in $\mathbb{B}$. The methodoly used is the following:

(IV.C.1) As previously explained, the mean modal density is calculated using a refined finite element model of the sound-insulation layer ($33,210$ DOF for the foam and $13,284$ DOF for the septum; there are $N = 1900$ elastic modes in the frequency band $]0, 450]$ Hz). The cut-off frequency Ω_C and the mean modal density $\underline{n}(\omega)$ are then deduced in the frequency band $\mathbb{B}$. We obtain $\Omega_C = 67 \times 2\pi\,\mathrm{rad.s}^{-1}$ and the graph of the smoothed function $\omega \mapsto \underline{n}(\omega)$ is given in Fig. 4 for frequency band $\mathbb{B}$. It should be noted that the modal density increases in the frequency band [250 , 300] Hz.

(IV.C.2) In the frequency band $[\omega_{min}, \Omega_C[$, we remind that the sound-insulation layer is equivalent to an added mass. The expression for the fuzzy coefficient $\underline{a}^s(\omega)$ is then $\underline{a}^s(\omega) = -\underline{\mu}\omega^2$ for $\omega < \Omega_C$. As explained in point (4.i) above, $\underline{\xi}$ is experimentally identified as the damping rate of the first elastic eigenmode of the structure with the sound-insulation layer. The identified values are $\underline{\xi} = 0.01$ and $\underline{\mu} = 5.9\,\mathrm{kg.m}^{-2}$.

(IV.C.3) We have chosen to directly identify the function $\omega \mapsto \nu(\omega)$ as explained

in points (4.iii) and (4.iv) above. The optimization problem consists in minimizing the distance between the model and the experiments for the FRF $\omega \mapsto r(\omega;\nu(\omega)) = 10\log_{10}\left(\sum_{i=1}^{n_{\rm obs}} |\gamma_i(\omega;\nu(\omega))|^2\right)$.

(IV.C.4) In the frequency band $[\omega_{min};\Omega_C[$, we have $\underline{\nu}(\omega) = 1$ and the modal density $\underline{n}(\omega)$ which is equal to zero. In the frequency band $[\Omega_C, \omega_{max}]$, we use the calculated mean modal density $\underline{n}(\omega)$ and the mean damping rate $\underline{\xi}$ in order to identify the mean coefficient of the participating mass $\underline{\nu}(\omega)$ as explained in point (4.iv) above. Figure 5 displays the updated mean coefficient $\underline{\nu}(\omega)$ of the participating mass and Fig. 6 shows the comparison between the experimental FRF and the FRF of the mean computational model for the structure with the sound-insulation layer calculated with the parameters experimentally identified.

(IV.C.5) The use of the structural part of the vibroacoustic model allows the identification of the mean parameters $\underline{\nu}(\omega)$, $\underline{\xi}$ and $\underline{n}(\omega)$. It should be noted that this identification allows not only the coefficient $\underline{a}^s(\omega)$ to be identified but also the coefficients $\underline{a}^c(\omega)$ and $\underline{a}^a(\omega)$. Therefore, we only need the structural part of the vibroacoustic model to identify all of the mean computational simplified model of the sound-insulation layer (*i.e.* the structural, the coupling and the acoustic parts).

V. COMPUTATIONAL STOCHASTIC MODEL FOR THE UNCERTAIN VIBROACOUSTIC SYSTEM INCLUDING THE SOUND-INSULATION LAYER

A. Stochastic vibroacoustic system

As we have explained in Section I, there are two sources of uncertainties. The first source is relative to the mean computational model of the structure without the sound-insulation layer coupled with the acoustic cavity. Concerning the structure *in vacuo*, Fig. 3 shows that the mean computational model gives a good enough prediction but some significant differences exist between the prediction and the experimental results. Consequently, the quality of the predictions of the mean computational model can be improved in implementing a

nonparametric probabilistic model of uncertainties to take into account both system parameters uncertainties and model uncertainties. Therefore, (1) the mean generalized matrices $[\underline{M}^s]$, $[\underline{D}^s(\omega)]$ and $[\underline{K}^s(\omega)]$ in Eq. (42) relative to the structure are replaced by the random matrices $[\mathbf{M}^s]$, $[\mathbf{D}^s(\omega)]$ and $[\mathbf{K}^s(\omega)]$, (2) the mean generalized matrices $[\underline{M}^a]$, $[\underline{D}^a(\omega)]$ and $[\underline{K}^a]$ in Eq. (43) relative to the acoustic cavity are replaced by the random matrices $[\mathbf{M}^a]$, $[\mathbf{D}^a(\omega)]$ and $[\mathbf{K}^a]$ and (3) the mean generalized coupling matrix $[\underline{C}]$ is replaced by the random matrix $[\mathbf{C}]$. The level of uncertainties of these random matrices is controlled by the dispersion parameters δ_{M^s}, δ_{D^s}, δ_{K^s}, δ_{M^a}, δ_{D^a}, δ_{K^a} and δ_C which are independent of the matrix dimension and of the frequency. The second source of uncertainties is introduced by the use of the simplified model of the sound-insulation layer based on the fuzzy structure theory. In fact, if this simplified model has the capability to predict in mean the effects of the sound-insulation layer on the structure and on the acoustic cavity, this simplified model does not describe the fluctuations around the mean value induced by these uncertainties. We then propose to use again the nonparametric probabilistic approach to take into account uncertainties in the simplified model. Consequently, the matrices $[\underline{B}^s]$, $[\underline{C}^s]$ and $[\underline{B}^a]$ of the mean simplified model of the sound-insulation layer are replaced by the random matrices $[\mathbf{B}^s]$, $[\mathbf{C}^s]$ and $[\mathbf{B}^a]$. The level of uncertainties of these random matrices is controlled by the dispersion parameters δ_{B^s}, δ_{C^s} and δ_{B^a} which are independent of the matrices dimension and of the frequency. The development of the construction of the probability model of all these random matrices with a nonparametric approach will not be detailed here. Such an approach is presented in Ref. [37, 40] and its application to a structural-acoustic system without sound-insulation layer can be found in Ref. [41, 42]. However, some details are given in Appendix D. Taking into account Eqs. (40), the vectors $\mathbf{U}^s(\omega)$ of the random structural displacement and $\mathbf{P}(\omega)$ of the random acoustic fluid pressure are written

$$\mathbf{U}^s(\omega) = [\underline{\Phi}^s]\mathbf{Q}^s(\omega) \quad , \quad \mathbf{P}(\omega) = [\underline{\Phi}^a]\mathbf{Q}^a(\omega) \quad . \tag{44}$$

The stochastic reduced computational vibroacoustic model can then be deduced and is written as, for all $\omega \in \mathbb{B}$,

$$\begin{bmatrix} [\mathbf{A}^s(\omega)] + \underline{a}^s(\omega)[\mathbf{B}^s] & [\mathbf{C}] + \underline{a}^c(\omega)[\mathbf{C}^s] \\ \omega^2\big\{[\mathbf{C}]^T + \underline{a}^c(\omega)[\mathbf{C}^s]^T\big\} & [\mathbf{A}^a(\omega)] + \underline{a}^a(\omega)[\mathbf{B}^a] \end{bmatrix} \times \begin{bmatrix} \mathbf{Q}^s(\omega) \\ \mathbf{Q}^a(\omega) \end{bmatrix} = \begin{bmatrix} \underline{\boldsymbol{f}}^s(\omega) \\ \underline{\boldsymbol{f}}^a(\omega) \end{bmatrix} \tag{45}$$

in which the random vectors $\mathbf{Q}^s(\omega)$ and $\mathbf{Q}^a(\omega)$ are the solution of the stochastic computational model and where the random matrices $[\mathbf{A}^s(\omega)]$ and $[\mathbf{A}^a(\omega)]$ are defined by Eqs. (D2) and (D3).

B. Solver for the stochastic reduced computational model

This section is devoted to the construction of the random solution of the stochastic computational model defined by Eq. (45). The stochastic solver is based on the use of the Monte Carlo method. The methodology used is then the following. For ω fixed in $\mathbb{B}$, (1) n_r independent realizations of the random variables $\mathbf{U}^s(\omega) = (U^s_1(\omega), \ldots, U^s_{m_s}(\omega))$ and $\mathbf{P}(\omega) = (P_1(\omega), \ldots, P_{m_a}(\omega))$ are constructed. For each realization $\mathbf{U}^s(\omega;\theta_\ell)$ and $\mathbf{P}(\omega;\theta_\ell)$ of the random vectors $\mathbf{U}^s(\omega)$ and $\mathbf{P}(\omega)$, the realizations of $R^s(\omega;\theta_\ell) = 10\log_{10}\left(\sum_{i=1}^{n_{\rm obs}} |\omega^2 U^s_{k_i}(\omega;\theta_\ell)|^2\right)$ and $R^a(\omega;\theta_\ell) = 10\log_{10}\left(\sum_{i=1}^{m_{\rm obs}} |P_{k_i}(\omega;\theta_\ell)|^2\right)$ are calculated in which $m_{\rm obs}$ is the number of pressure observations. (2) A convergence analysis is performed with respect to the number n_r of realizations and to the numbers n_s and n_a of modes. The order statistics and the method of quantiles (see Ref. [43]) are used to construct an estimation of the confidence regions of the observations.

C. Convergence analysis

For fixed values of the dispersion parameters, the convergence analysis with respect to n_r, n_s and n_a is carried out in studying the function,

$$(n_r, n_s, n_a) \mapsto \mathrm{Conv}^j(n_r, n_s, n_a) = \frac{1}{n_r} \sum_{\ell=1}^{n_r} \|\mathbf{Q}^j(\omega, \theta_\ell)\|^2, \tag{46}$$

with $j = s$ or a.

D. Estimation of the mean value and of the confidence region

Let $W(\omega)$ be the random variable representing $R^s(\omega)$ or $R^a(\omega)$. Let $F_{W(\omega)}(w)$ be the cumulative distribution function (continuous from the right) of the random variable $W(\omega)$, such that $F_{W(\omega)}(w) = P(W(\omega) \leq w)$. For $0 < p < 1$, the p^{th} quantile or fractile of $F_{W(\omega)}$ is defined as

$$\zeta(p) = \inf_{F_{W(\omega)}(w) \geq p} \{w\} \quad . \tag{47}$$

Then, the upper envelope $w_+(\omega)$ and the lower envelope $w_-(\omega)$ of the confidence region are defined by

$$w_+(\omega) = \zeta\left(\frac{1+P_c}{2}\right) \, , \, w_-(\omega) = \zeta\left(\frac{1-P_c}{2}\right) \, , \tag{48}$$

and are such that

$$\mathcal{P}(w_-(\omega) < W(\omega) \leq w_+(\omega)) = P_c \quad . \tag{49}$$

The estimation of $w_+(\omega)$ and $w_-(\omega)$ is performed by using the sample quantiles[43]. Let $w_1(\omega) = W(\omega; \theta_1), \ldots, w_{n_r}(\omega) = W(\omega; \theta_{n_r})$ be the n_r independent realizations of the random variable $W(\omega)$ computed as explained in section V. Let $\widetilde{w}_1(\omega) < \ldots < \widetilde{w}_{n_r}(\omega)$ be the order statistics associated with $w_1(\omega), \ldots, w_{n_r}(\omega)$. Therefore, one has the following estimation

$$w_+(\omega) \simeq \widetilde{w}_{j_+}(\omega), j_+ = \mathrm{fix}\,(n_r(1+P_c)/2) \quad , \tag{50}$$

$$w_-(\omega) \simeq \widetilde{w}_{j_-}(\omega), j_- = \mathrm{fix}\,(n_r(1-P_c)/2) \quad , \tag{51}$$

where fix(z) is the integer part of the real number z.

VI. IDENTIFICATION OF THE DISPERSION PARAMETERS OF THE PROBABILISTIC MODELS USING EXPERIMENTS - DESIGN METHODOLOGY PART 2

A. Convergence of the stochastic solver

In this section, we perform the experimental identification of the dispersion parameters δ_{M_s}, δ_{D_s} and δ_{K_s} for the structure and δ_{B_s} for the sound-insulation layer. This identification is carried out using the stochastic reduced computational model $[\mathbf{A}^s(\omega) + \underline{a}^s(\omega)[\mathbf{B}^s]]\,\mathbf{Q}^s(\omega) = \underline{\boldsymbol{f}}^s(\omega)$ for the structure coupled with the sound-insulation layer and not coupled with the acoustic cavity (see Eq. (45)). Consequently, for the largest possible values fixed at 0.8 of the dispersion parameters δ_{M_s}, δ_{D_s}, δ_{K_s} and δ_{B_s}, we need to calculate the values of the parameters n_r and n_s in order that the mean-square convergence is reached, *i.e.* in studying the function $(n_r, n_s) \mapsto \mathrm{Conv}^s(n_r, n_s)$. The graph of this function is shown in Fig. 7. It can be deduced that the convergence is reasonably reached for $n_s = 103$ modes and $n_r = 800$ realizations. Below, in the identification procedure presented, the parameters n_r and n_s are fixed to these values.

B. Description of the dispersion parameters identification

(i) In a first step, we use the experimental configuration (described in Section IV.A) in order to identify the dispersion parameters δ_{M_s}, δ_{D_s} and δ_{K_s} for the structure. The value of the damping dispersion parameter δ_{D_s} is fixed *a priori* to $\delta_{D_s} = 0.3$ according to the conclusion of Ref. [41]. In order to verify that the random response is not really sensitive[41] to the value of the parameter of dispersion δ_{D_s}, we have performed a sensitivity analysis with respect to δ_{D_s} varying in the interval $[0.2, 0.4]$ where δ_{M_s} and δ_{K_s} are fixed to the value 0.1 (small value of the dispersion parameter for the structural mass and stiffness matrices). With this sensitivity analysis, we have effectively verified that the influence of this dispersion parameter is negligible. Concerning the identification of the dispersion parameters δ_{M_s} and

δ_{K_s}, we use the maximum likelihood method with a statistical reduction method[45] (the method is recalled in Section VI.C) and we use[41,42] the assumption $\delta = \delta_{M_s} = \delta_{K_s}$. For this first step, Eq. (45) is then replaced by the random equation $[\mathbf{A}^s(\omega)]\,\mathbf{Q}^s(\omega) = \underline{\boldsymbol{f}}^s(\omega)$ relative to the uncertain structure without sound-insulation layer and without coupling with the acoustic cavity.

(ii) The second step is devoted to the identification of the dispersion parameter δ_{B_s} relative to the stochastic simplified model of the sound-insulation layer. Numerical simulations have shown that the sensitivity of the response of the structure coupled with the sound-insulation layer is smaller than the sensitivity of the response induced by the dispersion parameters of the structure. Consequently, the identification of δ_{B_s} cannot be carried out with the uncertain structure. Parameter δ_{B_s} must thus be identified with a "reference structure" for which there are no uncertainties (note that the sound-insulation layer cannot be analyzed alone and has to be coupled with a structure). The methodology proposed consists

(1) in defining a "reference structure" and analyzing the response of this "reference structure" coupled with the sound-insulation layer. This reference coupling system is analyzed by the finite element method using a fine mesh for the sound-insulation layer and the "reference structure". This deterministic computational model allows the responses to be computed. These responses are defined below as the "numerical experiments". Note that this computational model does not represent the experimental configuration, but this choice is completely coherent because the stochastic simplified model of the sound-insulation layer is independent of the choice of the structure. This model is constituted of a thin plate similar to the plate of the experimental configuration presented in Section IV.B;

(2) in constructing a stochastic computational model constituted of the computational model above for the "reference structure" and of the stochastic simplified model for the sound-insulation layer which depends on δ_{B_s}. The sound-insulation layer model is similar to the one presented in Section IV.B For this second step, Eq. (45) is then replaced by the random equation $[\underline{A}^s_{\text{ref}}(\omega) + \underline{a}^s(\omega)[\mathbf{B}^s]]\,\mathbf{Q}^s(\omega) = \underline{\boldsymbol{f}}^s(\omega)$.

The method then consists in minimizing the distance between the "numerical experiments" and the response of the stochastic reduced computational model. We then use again the maximum likelihood method with a statistical reduction.

C. Statistical reduction and maximum likelihood method

An efficient method has recently been proposed[45] to identify the dispersion parameters with the maximum likelihood method for a stochastic process such as the modulus of a FRF indexed by the frequency ω. This method consists in introducing a statistical reduction of the data and then applying the maximum likelihood method to the reduced random variables.
Firstly, we set the problem for both the steps described in points (i) and (ii) above. Secondly, we present the results for step 1 of point (i) above and thirdly, we simply give the results for step 2 of point (ii) above.

In this section, the optimization parameter is denoted by δ and represents the dispersion parameter $\delta_{M_s} = \delta_{K_s}$ or δ_{B_s}. For ω in band $\mathbb{B}$, let $\omega \mapsto W(\delta, \omega)$ be the second-order stochastic process defined on a probabilistic space $(\Theta, \mathcal{T}, \mathcal{P})$ which depends on the optimization parameter $\delta \in \Delta \subset \mathbb{R}$ and which represents the FRF $R^s(\delta, \omega)$ either for step 1 or step 2 defined in Section V.B. Let $\omega \mapsto W^{\exp}(\omega)$ be the experimental observation corresponding to the random observation $W(\delta, \omega)$ of the stochastic system. It should be noted that $W^{\exp}(\omega)$ represents either the experimental observation $W^{\exp}_{\text{step 1}}(\omega)$ of step 1 in point (i) or the reference calculation $W^{\text{ref}}_{\text{step 2}}(\omega)$ of step 2 in point (ii) above. Let $\{\omega_1, \ldots, \omega_{n_{\text{freq}}}\}$ be the frequency sampling of band $\mathbb{B}$.

Let $P_{W(\delta,\omega_1),\ldots,W(\delta,\omega_{n_{\text{freq}}})}(dw_1, \ldots, dw_{n_{\text{freq}}}, \delta)$ be the joint probability distribution on $\mathbb{R}^{n_{\text{freq}}}$

of random variables $W(\delta,\omega_1),\ldots,W(\delta,\omega_{n_{\rm freq}})$ depending on the dispersion parameter δ. For δ in Δ, this joint probability is assumed to be written as

$$\begin{aligned} &P_{W(\delta,\omega_1),\ldots,W(\delta,\omega_{n_{\rm freq}})}(dw_1,\ldots,dw_{n_{\rm freq}},\delta) \\ &\qquad = p(w_1,\ldots,w_{n_{\rm freq}},\delta)dw_1\ldots dw_{n_{\rm freq}} \end{aligned} \tag{52}$$

in which $p(w_1,\ldots,w_{n_{\rm freq}},\delta)$ is the probability density function on $\mathbb{R}^{n_{\rm freq}}$ with respect to the volume element $dw_1\ldots dw_{n_{\rm freq}}$. For all δ fixed in Δ and for all $w_1,\ldots,w_{n_{\rm freq}}$ given in $\mathbb{R}$, the estimation of $p(w_1,\ldots,w_{n_{\rm freq}},\delta)$ is performed by using the stochastic computational model and the Monte Carlo method (described in Section V.B) with n_r independent realizations $\{W(\delta,\omega_1,\theta_1),\ldots,W(\delta,\omega_{n_{\rm freq}},\theta_1)\},\ldots,\{W(\delta,\omega_1,\theta_{n_r}),\ldots,W(\delta,\omega_{n_{\rm freq}},\theta_{n_r})\}$ of the $\mathbb{R}^{n_{\rm freq}}$-valued random observation $\{W(\delta,\omega_1),\ldots,W(\delta,\omega_{n_{\rm freq}})\}$ with $\theta_1,\ldots,\theta_{n_r}$ in Θ. In practice, the sampling $\{\omega_1,\ldots,\omega_{n_{\rm freq}}\}$ of $\mathbb{B}$ is used and the experimental observation is

$$\{W^{\rm exp}(\omega_1),\ldots,W^{\rm exp}(\omega_{n_{\rm freq}})\} \quad . \tag{53}$$

The problem to be solved then is to find the optimal value $\delta^{\rm opt}$ of the dispersion parameter δ of the stochastic computational model using the experimental values defined by Eq. (53), such that

$$\delta^{\rm opt} = \arg\max_{\delta\in\Delta} \mathcal{L}(\delta) \quad , \tag{54}$$

with

$$\mathcal{L}(\delta) = \log_{10} p(W^{\rm exp}(\omega_1),\ldots,W^{\rm exp}(\omega_{n_{\rm freq}}),\delta)\,, \tag{55}$$

because there is only one experiment. Since $n_{\rm freq}$ is large (for instance $n_{\rm freq}=300$), the numerical cost to solve Eq. (54) is very high. A usual possible approximation consists in replacing the likelihood function $\mathcal{L}(\delta)$ by the following $\widetilde{\mathcal{L}}(\delta)=\sum_{k=1}^{n_{\rm freq}}\log_{10} p_{W(\delta,\omega_k)}(W^{\rm exp}(\omega_k),\delta)$ in which $p_{W(\delta,\omega_k)}$ is the probability density function of the random variable $W(\delta,\omega_k)$. This approximation is not efficient and gives an overestimation of $\delta^{\rm opt}$ due to the statistical dependence of $W(\delta,\omega_1),\ldots,W(\delta,\omega_{n_{\rm freq}})$. The method proposed[45] consists in the following methodology. Firstly, a statistical reduction of information using a principal component analysis is performed and secondly, the maximum likelihood method is applied in the space

of the uncorrelated random variables related to the reduced statistical information. For all δ in Δ, we define the random vectors $\mathbb{W}(\delta) = (W(\delta,\omega_1),\ldots,W(\delta,\omega_{n_{\rm freq}}))$, $\mathbb{m}(\delta) = \mathcal{E}\{\mathbb{W}(\delta)\}$ and $\mathbb{W}^{\rm exp} = (W^{\rm exp}(\omega_1),\ldots,W^{\rm exp}(\omega_{n_{\rm freq}}))$. Let $[C_{\mathbb{W}}(\delta)]$ be the $(n_{\rm freq}\times n_{\rm freq})$ covariance matrix defined by

$$[C_{\mathbb{W}}(\delta)] = \mathcal{E}\big\{(\mathbb{W}(\delta)-\mathbb{m}(\delta))(\mathbb{W}(\delta)-\mathbb{m}(\delta))^T\big\} \quad , \tag{56}$$

where $\mathbb{m}(\delta)$ and $[C_{\mathbb{W}}(\delta)]$ are estimated with the Monte Carlo method. We introduce the eigenvalue problem

$$[C_{\mathbb{W}}(\delta)]\mathbb{x}(\delta) = \lambda(\delta)\mathbb{x}(\delta) \tag{57}$$

for which the positive eigenvalues are such that $\lambda_1(\delta) \geq \lambda_2(\delta) \geq \ldots \geq \lambda_{n_{\rm freq}}(\delta)$. The corresponding vectors $\mathbb{x}^1(\delta),\mathbb{x}^2(\delta),\ldots,\mathbb{x}^{n_{\rm freq}}(\delta)$ are orthonormal in $\mathbb{R}^{n_{\rm freq}}$ and are written as $\mathbb{x}^\alpha(\delta) = (x^{\alpha 1}(\delta),\ldots,x^{\alpha n_{\rm freq}}(\delta))$. Let $N_{\rm red}$ be an integer lesser than $n_{\rm freq}$. We can then introduce the approximation $\mathbb{W}^{N_{\rm red}}(\delta)$ of $\mathbb{W}(\delta)$ defined by

$$\mathbb{W}^{N_{\rm red}}(\delta) = \mathbb{m}(\delta) + \sum_{\alpha=1}^{N_{\rm red}} \sqrt{\lambda_\alpha(\delta)}\, Y_\alpha(\delta)\, \mathbb{x}^\alpha(\delta) \tag{58}$$

in which $Y_1(\delta),\ldots,Y_{N_{\rm red}}(\delta)$ are $N_{\rm red}$ real-valued uncorrelated random variables such that, for all $\alpha = 1,\ldots,N_{\rm red}$,

$$Y_\alpha(\delta) = \frac{1}{\sqrt{\lambda_\alpha(\delta)}} < \mathbb{W}(\delta) - \mathbb{m}(\delta)\,,\, \mathbb{x}^\alpha(\delta) >_{\mathbb{B}} \quad , \tag{59}$$

where $<\,.\,,\,.\,>_{\mathbb{B}}$ is the euclidian inner product on $\mathbb{R}^{n_{\rm freq}}$ and $||.||_{\mathbb{B}}$ is its associated norm. Let $|||.|||$ be the norm defined by $|||W|||^2 = \mathcal{E}\{||W||^2_{\mathbb{B}}\}$. The order $N_{\rm red}$ of the statistical reduction is calculated to get an approximation with a given accuracy ε independent of $N_{\rm red}$ and δ, such that $\max_\delta\{|||\mathbb{D}-\mathbb{D}^{\rm red}|||^2/|||\mathbb{D}|||^2\} \leq \varepsilon$ with $\mathbb{D} = \mathbb{W}(\delta)-\mathbb{m}(\delta)$ and $\mathbb{D}^{\rm red} = \mathbb{W}^{N_{\rm red}}(\delta)-\mathbb{m}(\delta)$. The value of $N_{\rm red}$ has then to be such that,

$$\max_{\delta\in\Delta}\left(1 - \frac{\sum_{\alpha=1}^{N_{\rm red}}\lambda_\alpha(\delta)}{{\rm tr}[C_{\mathbb{W}}(\delta)]}\right) \leq \varepsilon \quad . \tag{60}$$

The statistical reduction is efficient when $N_{\rm red} \ll n_{\rm freq}$.

Let $(y_1, \ldots, y_{N_{\rm red}}) \mapsto p_{Y_1(\delta),\ldots,Y_{N_{\rm red}}(\delta)}(y_1, \ldots, y_{N_{\rm red}}, \delta)$ be the probability density function on $\mathbb{R}^{N_{\rm red}}$ with respect to $dy_1, \ldots, dy_{N_{\rm red}}$ of the uncorrelated (but not independent) random variables $Y_1(\delta), \ldots, Y_{N_{\rm red}}(\delta)$. From Eq. (59), it can be deduced that, for all α in $\{1, \ldots, N_{\rm red}\}$, the experimental realization $Y_\alpha^{\rm exp}(\delta)$ which now depends on δ is given, for all $\alpha = 1, \ldots, N_{\rm red}$, by

$$Y_\alpha^{\rm exp}(\delta) = \frac{1}{\sqrt{\lambda_\alpha(\delta)}} < \mathbb{W}^{\rm exp} - \mathbb{m}(\delta) \, , \, \mathbb{x}^\alpha(\delta) >_{\mathbb{B}} \quad . \tag{61}$$

Let $\widetilde{\mathcal{L}}^{\rm red}$ be the following approximation of the reduced log-likelihood function which is defined, for all δ fixed in Δ, by

$$\widetilde{\mathcal{L}}^{\rm red}(\delta) = \sum_{\alpha=1}^{N_{\rm red}} \log_{10} p_{Y_\alpha(\delta)}(Y_\alpha^{\rm exp}(\delta), \delta) \tag{62}$$

in which $y \mapsto p_{Y_\alpha(\delta)}(y, \delta)$ is the probability density function on $\mathbb{R}$ of the real-valued random variable $Y_\alpha(\delta)$. This approximation would be exact if the random variables $Y_1(\delta), \ldots, Y_{N_{\rm red}}(\delta)$ were mutually independent and so the joint probability density function could be written as the product of the marginal probability density functions which is not true in the present case. Nevertheless, this approximation is reasonably good because the centered random variables $Y_1(\delta), \ldots, Y_{N_{\rm red}}(\delta)$, although they are mutually dependent, are uncorrelated. The optimization problem to be solved is then given by the following one,

$$\delta^{\rm opt} = \arg\max_{\delta \in \Delta} \widetilde{\mathcal{L}}^{\rm red}(\delta) \quad . \tag{63}$$

D. Summary of the identification method

From the experimental measurements $W^{\rm exp}(\omega_1), \ldots, W^{\rm exp}(\omega_{n_{\rm freq}})$ and using Eq. (61) yield the values $Y_1^{\rm exp}(\delta), \ldots, Y_{N_{\rm red}}^{\rm exp}(\delta)$, for all δ in Δ. The use of the stochastic computational model and the Monte Carlo method allows to compute independent realizations of the dependent random variables $W(\delta, \omega_1), \ldots, W(\delta, \omega_{n_{\rm freq}})$, for all δ in Δ. For a fixed accuracy parameter ε, the smallest value of $N_{\rm red} \leq n_{\rm freq}$ is calculated with the use of Eq. (60). The use of Eq. (59) then allows the independent realizations of the dependent but uncorrelated random variables $Y_1(\delta), \ldots, Y_{N_{\rm red}}(\delta)$ to be calculated and to deduce estimations of the

marginal probability density function $p_{Y_\alpha(\delta)}(Y_\alpha^{\exp}(\delta), \delta)$. Using Eqs. (62) and (63) yields the optimized dispersion parameter δ^{opt}.

E. Results

This section is devoted to the identification of the dispersion parameters δ_{M_s} and δ_{K_s} of the structure according to step 1 of point (i) of Section VI.B. We then perform the identification of the dispersion parameter δ_{B_s} for the sound-insulation layer according to step 2 of point (ii) of Section VI.B. First, Eq. (60) is used with $\Delta = [0.1, 0.95]$ to compute the value of N_{red} and yields $N_{\text{red}} = 100$ for $\varepsilon = 0.02$. Figure 8 displays the graph of the function $\delta \mapsto \widetilde{\mathcal{L}}^{\text{red}}(\delta)$ for $N_{\text{red}} = 100$. The maximum of this function is reached for $\delta_{M_s}^{\text{opt}} = \delta_{K_s}^{\text{opt}} = \delta^{\text{opt}} = 0.3$. Figure 9 displays the graph of the FRF $\omega \mapsto R^s(\omega)$ defined in Section V.B for the uncertain structure without the sound-insulation layer and with $\delta_{D_s} = 0.3$.

The identification of the dispersion parameter δ_{B_s} is performed as explained is Section VI.B (ii). For the sake of brevity, we only give the result obtained from the optimization problem which is $\delta_{B_s}^{\text{opt}} = 0.6$. Figure 10 displays the graph of the FRF $\omega \mapsto R^s(\omega)$ defined in Section V.B for the uncertain structure coupled with the uncertain sound-insulation layer and with $\delta_{D_s} = 0.3$.

The confidence region is computed with a probability level of 95 % and then the probability that the experiments be outside the confidence region is non zero. Certainly, this prediction could be improved both in increasing the number of realizations and in improving the underlying deterministic model of the structure without the sound-insulation layer.

VII. PREDICTION OF THE VIBROACOUSTIC RESPONSES WITH THE IDENTIFIED COMPUTATIONAL STOCHASTIC MODEL

In this section, we use the identified computational stochastic model to predict a vibroacoustic response. The response of the identified model is compared to a reference solution calculated with a commercial software. The structure and the sound-insulation layer models are defined in Section IV. The sound-insulation layer is coupled with a parallelepipedic acoustic cavity ($m_a = 23,354$ DOF and $n_a = 67$ modes) which is assumed to be without uncertainties and which is filled with air. Firstly, we observe the pressure at $m_{\rm obs} = 120$ points in the acoustic cavity while the excitation force is applied to the elastic framework of the structure as in Section IV. We then compute the FRF $\omega \mapsto r^a(\omega)$ relative to the acoustic cavity and Fig. 11 displays its graph for the mean acoustic system with and without the sound-insulation layer. This figure shows the effects of the sound-insulation layers of the vibroacoustic responses of the reference configuration. It can be seen that there is a significant effect on frequency band [200,450] Hz. Secondly, we use the same observation in the acoustic cavity and the same structural excitation as above. Uncertainties are now taken into account in the structure and in the sound-insulation layer. The random equation which has to be solved is then the following,

$$\left[\begin{array}{cc} [\mathbf{A}^s(\omega)] + \underline{a}^s(\omega)[\mathbf{B}^s] & \underline{a}^c(\omega)[\mathbf{C}^s] \\ \omega^2\, \underline{a}^c(\omega)[\mathbf{C}^s]^T & [\underline{A}^a(\omega)] + \underline{a}^a(\omega)[\mathbf{B}^a] \end{array}\right] \times \left[\begin{array}{c} \mathbf{Q}^s(\omega) \\ \mathbf{Q}^a(\omega) \end{array}\right] = \left[\begin{array}{c} \underline{\boldsymbol{f}}^s(\omega) \\ \underline{\boldsymbol{f}}^a(\omega) \end{array}\right] . \tag{64}$$

The values of the dispersion parameters of the probabilistic model are the values identified in Section VI.E, *i.e.* $\delta_{M_s}^{\rm opt} = \delta_{K_s}^{\rm opt} = 0.3$, $\delta_{D_s} = 0.3$ and $\delta_{B_a}^{\rm opt} = 0.6$. It is assumed that the dispersion parameters for the sound-insulation layer are equal, that is to say $\delta_{C_s}^{\rm opt} = \delta_{B_a}^{\rm opt} = \delta_{B_s}^{\rm opt} = 0.6$. Figure 12 defined in Section V.B for the uncertain structure coupled with the uncertain sound-insulation layer and the acoustic cavity. The analysis of this figure shows

that there are differences between the reference response (thick solid line) and the response of the mean simplified computational model (these differences can be estimated looking at the statistical mean response given by the mid-grey line). Nevertheless, the stochastic simplified computational model allows the prediction to be improved in the probability sense. It can be seen that the reference response belongs to the confidence region. Firstly, the two responses coincide in the frequency band [0,40] Hz. Secondly, it can be seen that the reference solution is close to the lower bound of the confidence region in the frequency band [40,250] Hz. Finally, the reference solution reaches the lower- and the upper-envelopes of the confidence in the frequency-band [250,450] Hz.

VIII. CONCLUSION

In this paper, a new extension of the fuzzy structure theory to elastoacoustic element is presented in order to construct a simplified model of sound-insulation layers. Such a simplified model, based on an extension of the fuzzy structure theory, (1) allows the dynamics of the sound-insulation layer to be taken into account without increasing the number of DOF in the computational vibroacoustic model and (2) allows a representation of the sound-insulation in terms of physical parameters such as its participating mass, its modal density and its internal damping rate. This approach allows several kinds of sound-insulation layers to be simultaneously taken into account in the computational vibroacoustic model of a complex system such as a car with a very small increase of the computational cost. In addition, taking into account the complexity of the actual sound-insulation layers design, it is necessary to implement a model of uncertainties. This is a reason why a probabilistic approach of both model and system parameters uncertainties is introduced in the simplified model of the sound-insulation layer based on the fuzzy structure theory. The complete related developments are given and an experimental validation is presented. Figure 10 (relative to the response of the structure coupled with the sound-insulation layer) and Fig. 12 (relative to the response of the acoustic cavity for the vibroacoustic system constituted of the structure cou-

pled with the sound-insulation layer and with the acoustic cavity) show that the predictions are good from a stochastic point of view. Finally, an efficient design methodology is proposed to identify the parameters of the simplified model of the sound-insulation layer. The mean parameters are identified by solving an inverse problem formulated as an optimization problem using an experimental database. The maximum likelihood method coupled to a statistical reduction of information is performed to obtain the dispersion parameters.

The method proposed in this paper is not intended to give a tool for designing sound-insulation layers (which are designed using high-frequency responses considerations). This approach has been developed in the low- and medium-frequency bands in complex structural-acoustics systems like cars for which, due to industrial processes and vehicle diversity, there are very large variabilities induced by the kinematic conditions at the attachment interface between the master structure and the sound-insulation layers.

Acknowledgments

This research has been supported by the french agency for research and technology (ANRT).

APPENDIX A: FORMULATION OF THE VIBROACOUSTIC PROBLEM WITH A SOUND-INSULATION LAYER

In this section, we give additional explanations relative to Section II useful for the construction of the simplified model of the sound-insulation layer. Let $\mathcal{C}_0^s$ be the space of the admissible displacement fields of the structure, $\mathcal{C}^a$ be the space of the admissible pressure fields in the acoustic cavity and $\mathcal{C}^h$ be the space of the admissible displacement fields of the sound-insulation layer. For all ω in $\mathbb{B}$, we introduce the following bilinear form defined on $\mathcal{C}_0^s \times \mathcal{C}^a$,

$$c_{\Gamma_2}(\boldsymbol{u}^s, p) = \int_{\Gamma_2} \boldsymbol{u}^s(\boldsymbol{x}).\boldsymbol{n}^s(\boldsymbol{x})\, p(\boldsymbol{x})\, ds(\boldsymbol{x}) \quad , \tag{A1}$$

the bilinear form defined on $\mathcal{C}^h \times \mathcal{C}^a$,

$$c_{\Gamma}(\boldsymbol{u}^h, p) = \int_{\Gamma} \boldsymbol{u}^h(\boldsymbol{x}).\boldsymbol{n}(\boldsymbol{x})\, p(\boldsymbol{x})\, ds(\boldsymbol{x}) \quad , \tag{A2}$$

and the linear form defined on $\mathcal{C}_0^s$ or $\mathcal{C}^h$,

$$c_{\Gamma_s}(\boldsymbol{u}; \omega) = \int_{\Gamma_s} \boldsymbol{f}^s(\boldsymbol{x}, \omega)\, \boldsymbol{u}(\boldsymbol{x})\, ds(\boldsymbol{x}) \quad . \tag{A3}$$

The weak formulation of the vibroacoustic boundary value problem is formulated as follows (see Ref. [12]). For all ω in $\mathbb{B}$, find $(\boldsymbol{u}^s, p, \boldsymbol{u}^h)$ in $\mathcal{C}_0^s \times \mathcal{C}^a \times \mathcal{C}^h$ such that for all $(\boldsymbol{\delta u}^s, p, \boldsymbol{\delta u}^h)$ in $\mathcal{C}_0^s \times \mathcal{C}^a \times \mathcal{C}^h$, we have, for the structure,

$$\begin{aligned} -\omega^2 m^s(\boldsymbol{u}^s, \boldsymbol{\delta u}^s) + i\omega\, d^s(\boldsymbol{u}^s, \boldsymbol{\delta u}^s; \omega) + k^s(\boldsymbol{u}^s, \boldsymbol{\delta u}^s; \omega) & \\ + c_{\Gamma_2}(\boldsymbol{\delta u}^s, p) = -c_{\Gamma_s}(\boldsymbol{\delta u}^s; \omega) + l^s(\boldsymbol{\delta u}^s; \omega) \quad , & \end{aligned} \tag{A4}$$

for the acoustic cavity,

$$\begin{aligned} -\omega^2 m^a(p, \delta p) + i\omega\, d^a(p, \delta p; \omega) + k^a(p, \delta p) & \\ + \omega^2 \left\{ c_{\Gamma_2}(\boldsymbol{u}^s, \delta p) + c_{\Gamma}(\boldsymbol{u}^h, \delta p) \right\} = l^a(\delta p; \omega) \quad , & \end{aligned} \tag{A5}$$

and for the sound-insulation layer,

$$\begin{aligned} -\omega^2 m^h(\boldsymbol{u}^h, \boldsymbol{\delta u}^h) + i\omega\, d^h(\boldsymbol{u}^h, \boldsymbol{\delta u}^h; \omega) + k^h(\boldsymbol{u}^h, \boldsymbol{\delta u}^h; \omega) & \\ c_{\Gamma}(\boldsymbol{\delta u}^h, p) = c_{\Gamma_s}(\boldsymbol{\delta u}^h; \omega) \quad . & \end{aligned} \tag{A6}$$

The bilinear forms m^s, d^s, k^s, (respectively m^a, d^a, k^a and respectively m^h, d^h, k^h) relative to the mass, damping and stiffness of the structure (respectively of the acoustic cavity and respectively of the sound-insulation layer) and the linear forms l^s and l^a related to the

structural and acoustical excitations are defined in Ref. [12]. For instance, we have

$$m^s(\boldsymbol{u}^s,\boldsymbol{\delta u}^s)=\int_{\Omega_s}\rho^s(\boldsymbol{x})\boldsymbol{u}^s(\boldsymbol{x}).\boldsymbol{\delta u}^s(\boldsymbol{x})d\boldsymbol{x}\quad , \tag{A7}$$

$$d^s(\boldsymbol{u}^s,\boldsymbol{\delta u}^s;\omega)=\int_{\Omega_s}b_{ijkh}(\boldsymbol{x},\omega)\varepsilon_{kh}(\boldsymbol{u}^s)\varepsilon_{ij}(\boldsymbol{\delta u}^s)d\boldsymbol{x}, \tag{A8}$$

$$k^s(\boldsymbol{u}^s,\boldsymbol{\delta u}^s;\omega)=\int_{\Omega_s}a_{ijkh}(\boldsymbol{x},\omega)\varepsilon_{kh}(\boldsymbol{u}^s)\varepsilon_{ij}(\boldsymbol{\delta u}^s)\,d\boldsymbol{x}, \tag{A9}$$

$$m^a(p,\delta p)=\frac{1}{\rho_0 c_0^2}\int_{\Omega_a}p(\boldsymbol{x})\delta p(\boldsymbol{x})\,d\boldsymbol{x}\quad , \tag{A10}$$

$$d^a(p,\delta p;\omega)=\tau(\omega)\,k^a(p,\delta p)\quad , \tag{A11}$$

$$k^a(p,\delta p)=\frac{1}{\rho_0}\int_{\Omega_a}\boldsymbol{\nabla}p.\boldsymbol{\nabla}\delta p\,d\boldsymbol{x}\quad , \tag{A12}$$

$$c_{\Gamma_2}(\boldsymbol{u}^s,\delta p)=\int_{\Gamma_2}\boldsymbol{u}^s(\boldsymbol{x}).\boldsymbol{n}^s(\boldsymbol{x})\,\delta p(\boldsymbol{x})\,ds(\boldsymbol{x})\quad . \tag{A13}$$

APPENDIX B: FUNCTIONS OF THE FUZZY COEFFICIENTS INTRODUCED IN SECTION II.E

For all $\omega\in[\Omega_C,\omega_{\max}]$,

$$\Theta_{\scriptscriptstyle R}(\omega)= \tag{B1}$$

$$\frac{1}{4\sqrt{1-\underline{\xi}(\omega)^2}}\ln\left\{\frac{N^+(\widetilde{b}(\omega),\underline{\xi}(\omega))\,N^-(\widetilde{a}(\omega),\underline{\xi}(\omega))}{N^-(\widetilde{b}(\omega),\underline{\xi}(\omega))\,N^+(\widetilde{a}(\omega),\underline{\xi}(\omega))}\right\}, \tag{B2}$$

$$\Theta_{\scriptscriptstyle I}(\omega)=$$

$$\frac{1}{2\sqrt{1-\underline{\xi}(\omega)^2}}\left[\Lambda(\widetilde{b}(\omega),\underline{\xi}(\omega))-\Lambda(\widetilde{a}(\omega),\underline{\xi}(\omega))\right], \tag{B3}$$

$$N^{\pm}(u,\xi)=u^2\pm 2\,u\,\sqrt{1-\xi^2}+1\quad , \tag{B4}$$

$$\Lambda(u,\xi)=\arctan\left\{\frac{u^2+2\xi^2-1}{2\xi\sqrt{1-\xi^2}}\right\}\quad , \tag{B5}$$

$$\widetilde{a}(\omega)=\frac{1}{\omega}a(\omega)\quad \text{, where } a \text{ is defined in Eq. (14)}\quad , \tag{B6}$$

$$\widetilde{b}(\omega)=\frac{1}{\omega}b(\omega)\quad \text{, where } b \text{ is defined in Eq. (15)}\quad , \tag{B7}$$

$$\widetilde{\ell}(\omega)=\frac{1}{\widetilde{b}(\omega)-\widetilde{a}(\omega)}\quad ,\ \underline{\lambda}(\omega)=\frac{\widetilde{\ell}(\omega)}{\omega\underline{n}(\omega)}\quad . \tag{B8}$$

APPENDIX C: GRAPHS OF THE FUZZY COEFFICIENTS

Figs. 13 to 18 display the graphs of the fuzzy coefficients defined by Eqs. (29) to (34) with Eqs. (B1) to (B8) for $\underline{\xi} = 0.01$, $\underline{n}(\omega)$ given by Fig. 4 and $\underline{\nu}(\omega)$ given by Fig. 5.

APPENDIX D: COMPLEMENTS RELATIVE TO THE NONPARAMETRIC PROBABILISTIC APPROACH

This section deals with complements relative to the probabilistic nonparametric approach which allows both model and system parameters uncertainties to be taken into account in the computational model of the structure, in the simplified model of the sound-insulation layer and in the computational model of the acoustic cavity. The random matrices associated with $[\underline{M}^s]$, $[\underline{D}^s(\omega)]$, $[\underline{K}^s(\omega)]$, $[\underline{C}]$, $[\underline{M}^a]$, $[\underline{D}^a(\omega)]$, $[\underline{K}^a]$, $[\underline{B}^s]$, $[\underline{B}^a]$ and $[\underline{C}^s]$ are constructed as explained in Ref. [40]. In this construction, the complex coefficients $\underline{a}^s(\omega)$, $\underline{a}^a(\omega)$ and $\underline{a}^c(\omega)$ are deterministic. For example, the random matrix associated with $\underline{a}^s(\omega)[\underline{B}^s]$ is $\underline{a}^s(\omega)[\mathbf{B}^s]$ in which $[\mathbf{B}^s]$ is the random matrix associated with $[\underline{B}^s]$. For ω fixed in $\mathbb{B}$, we then introduce the matrices $[\mathbf{M}^s]$, $[\mathbf{D}^s(\omega)]$, $[\mathbf{K}^s(\omega)]$, $[\mathbf{C}]$, $[\mathbf{M}^a]$, $[\mathbf{D}^a(\omega)]$, $[\mathbf{K}^a]$, $[\mathbf{B}^s]$, $[\mathbf{C}^s]$ and $[\mathbf{B}^a]$. These matrices are independent second-order random variables. The random matrices $[\mathbf{M}^s]$, $[\mathbf{D}^s(\omega)]$ and $[\mathbf{K}^s(\omega)]$ are with values in $\mathbb{M}_{n_s}^+(\mathbb{R})$; the random matrix $[\mathbf{B}^s]$ is with values in $\mathbb{M}_{n_s}^{+0}(\mathbb{R})$; the random matrix $[\mathbf{M}^a]$ is with values in $\mathbb{M}_{n_a}^+(\mathbb{R})$; the random matrices $[\mathbf{K}^a]$, $[\mathbf{D}^a(\omega)]$ and $[\mathbf{B}^a]$ are with values in $\mathbb{M}_{n_a}^{+0}(\mathbb{R})$ and the random matrices $[\mathbf{C}]$ and $[\mathbf{C}^s]$ are with values in $\mathbb{M}_{n_s,n_a}(\mathbb{R})$. The mean values of these random matrices are such that

$$
\begin{aligned}
&\mathcal{E}\{[\mathbf{M}^s]\} = [\underline{M}^s]\,, && \mathcal{E}\{[\mathbf{D}^s(\omega)]\} = [\underline{D}^s(\omega)]\,,\\
&\mathcal{E}\{[\mathbf{K}^s(\omega)]\} = [\underline{K}^s(\omega)]\,, && \mathcal{E}\{[\mathbf{M}^a]\} = [\underline{M}^a]\,,\\
&\mathcal{E}\{[\mathbf{D}^a(\omega)]\} = [\underline{D}^a(\omega)]\,, && \mathcal{E}\{[\mathbf{K}^a]\} = [\underline{K}^a]\,,\\
&\mathcal{E}\{\underline{a}^s(\omega)[\mathbf{B}^s]\} = \underline{a}^s(\omega)[\underline{B}^s]\,, && \mathcal{E}\{[\mathbf{C}]\} = [\underline{C}]\,,\\
&\mathcal{E}\{\underline{a}^a(\omega)[\mathbf{B}^a]\} = \underline{a}^a(\omega)[\underline{B}^a]\,, && \mathcal{E}\{\underline{a}^c(\omega)[\mathbf{C}^s]\} = \underline{a}^c(\omega)[\underline{C}^s],
\end{aligned}
\tag{D1}
$$

where $\mathcal{E}$ is the mathematical expectation. Moreover, those matrices have the required mathematical properties (see Ref. [39, 40] in which the reader will be able to find all the details). The generalized stiffness random matrices are then written as,

$$[\mathbf{A}^s(\omega)] = -\omega^2\ [\mathbf{M}^s] + i\omega\ [\mathbf{D}^s(\omega)] + [\mathbf{K}^s(\omega)] \quad , \tag{D2}$$

$$[\mathbf{A}^a(\omega)] = -\omega^2\ [\mathbf{M}^a] + i\omega\ [\mathbf{D}^a(\omega)] + [\mathbf{K}^a] \quad , \tag{D3}$$

where $[\mathbf{A}^s(\omega)]$ is a random matrix with values in $M_{n_s}^S(\mathbb{C})$ and where $[\mathbf{A}^a(\omega)]$ is a random matrix with values in $M_{n_a}^S(\mathbb{C})$. For example, we give below the detail of the construction for the random matrix $[\mathbf{K}^s(\omega)]$. The matrix $[\underline{K}^s(\omega)]$ can be written as $[\underline{K}^s(\omega)] = [L_{K^s}(\omega)]^T[L_{K^s}(\omega)]$ corresponding to the Choleski decomposition of the positive-definite matrix $[\underline{K}^s(\omega)]$. We then introduce the random matrix $[\mathbf{K}^s(\omega)] = [L_{K^s}(\omega)]^T[\mathbf{G}_{K^s}][L_{K^s}(\omega)]$ where the random matrix $[\mathbf{G}_{K^s}]$ belongs to the $\mathbf{SG}^+$ ensemble defined in Ref. [40] and is independent of the frequency. The dispersion parameter δ_{K^s} of this random matrix $[\mathbf{K}^s(\omega)]$ is independent of the dimension and of the frequency and is defined as by $\delta_{K^s} = (\mathcal{E}\{\|[\mathbf{G}_{K^s}] - [\underline{G}_{K^s}]\|_F^2\}/\|[\underline{G}_{K^s}]\|_F^2)^{1/2}$ in which $\|K\|_F$ is the Frobenius norm defined by $\|K\|_F^2 = \mathrm{tr}(K^TK)$.

REFERENCES

[1] Y.-J. Kang and J.S. Bolton, "Finite element modeling of isotropic elastic porous materials coupled with acoustical finite elements", J. Acoust. Soc. Am., **98**, 635–643 (1995).

[2] Y.-J. Kang and J.S. Bolton, "A finite element model for sound transmission through foam-lined double-panel structures", J. Acoust. Soc. Am., **99**, 2755–2765, (1996).

[3] R. Panneton and N. Atalla, "Numerical prediction of sound transmission through finite multilayer systems with poroelastic materials", J. Acoust. Soc. Am., **100**, 346–354 (1996).

[4] R. Panneton and N. Atalla, "An efficient finite element scheme for solving the three-dimensional poroelasticity problem in acoustics", J. Acoust. Soc. Am., **101**, 3287–3298 (1997).

[5] N. Atalla, R. Panneton and P. Debergue, "A mixed displacement-pressure formulation for poroelastic materials", J. Acoust. Soc. Am., **104**, 1444–1452 (1998).

[6] N. Atalla, M. A. Hamdi and R. Panneton, "Enhanced weak integral formulation for the mixed (u,p) poroelastic equations", J. Acoust. Soc. Am., **109**, 3065–3068 (2001).

[7] N. Atalla, F. Sgard and C. K. Amedin, "On the modeling of sound radiation from poroelastic materials", J. Acoust. Soc. Am., **120**, 1990–1995 (2006).

[8] F. J. Fahy, *Sound and Structural Vibration, Radiation, Transmission and Response* (Academic, New York, 1985).

[9] A.D. Pierce, *Acoustics: An Introduction to its Physical Principles and Applications* (originally published in 1981, McGraw-Hill Acoust. Soc. Am., Publications on Acoustics, Woodbury, 1989).

[10] M.C. Junger and D. Feit, *Sound, Structures, and Their Interaction* (originally published in 1972, Acoustical Society of America, New York, 1993).

[11] J.F Allard, *Propagation of Sound in Porous Media: Modelling Sound Absorbing Materials* (Chapman and Hall, London, 1994).

[12] R. Ohayon and C. Soize, *Structural Acoustics and Vibration* (Academic press, San Diego, 1998).

[13] J.L. Guyader and C. Lesueur, "Acoustic transmission through orthotropic multilayered plates, part. I. Plate vibration modes", J. Sound Vib., **58**, 51–86 (1978).

[14] J. A. Moore and R. H. Lyon, "Resonant porous material absorbers", J. Acoust. Soc. Am., **72**, 1989–1999 (1982).

[15] J.F. Allard, C. Champoux and C. Depollier, "Modelization of layered sound absorbing materials with transfer matrices", J. Acoust. Soc. Am., **82**, 1792–1796 (1987).

[16] A. Blaise, C. Lesueur, M. Gotteland and M. Barbe, "On sound transmission into an orthotropic infinite shell - Comparison with Koval's results and understanding of phenomena", J. Sound Vib., **150**, 233–243 (1991).

[17] J.-F. Allard and G. Daigle, "Propagation of Sound in Porous Media: Modeling Sound Absorbing Materials", J. Acoust. Soc. Am., **95**, 2785 (1994).

[18] C. Lesueur, G. Poumerol and A. Blaise, "Vibroacoustic response of composite multilayered plate coupled to a rectangular cavity and excited by white noise and a turbulent boundary layer", Acta Acustica, **3**, 153–167 (1995).

[19] N. Atalla and R. Panneton, "The effects of multilayer sound-absorbing treatments on the noise field inside a plate backed-cavity", J. Noise Control Eng., **44**, 235–243 (1996).

[20] R. S. Langley and P. Bremner, "A hybrid method for the vibration analysis of complex structural-acoustic systems", J. Acoust. Soc. Am., **105**, 1657–1671 (1999).

[21] J.M. Cushieri and D. Feit, "Influence of circumferential partial coating on the acoustic radiation from a fluid-loaded shell", J. Acoust. Soc. Am., **107**, 3196–3207 (2000).

[22] B. Faverjon and C. Soize, "Equivalent acoustic impedance model. Part 2: analytical approximation", J. Sound Vib., **276**, 593–613 (2004).

[23] L. Jaouen, B. Brouard, N. Atalla and C. Langlois, "A simplified numerical model for a plate backed by a thin foam layer in the low frequency range", J. Sound Vib., **280**, 681–698 (2005).

[24] C. Soize, "Probabilistic structural modeling in linear dynamical analysis of complex mechanical systems. I. Theoretical elements", Rech. Aerosp. **5**, 23–48 (1986). (English edition).

[25] F. Chabas, A. Desanti and C. Soize, "Probabilistic structural modeling in linear dynamical analysis of complex mechanical systems. II. Numerical analysis and applications", Rech. Aerosp. **5**, 49–67 (1986). (English edition).

[26] C. Soize, "A model and numerical method in the medium frequency range for vibroacoustic predictions using the theory of structural fuzzy", J. Acoust. Soc. Am., **94**, 849–865 (1993).

[27] C. Soize, "Estimation of the fuzzy substructure model parameters using the mean power flow equation of the fuzzy structure", Journal of Vibration and Acoustics, **120**, 279–286 (1998).

[28] C. Soize and K. Bjaoui, "Estimation of fuzzy structure parameters for continuous junctions", Journal of Vibration and Acoustic, J. Sound Vib., **107**, 2011–2020 (2000).

[29] A. D. Pierce, V. W. Sparrow and D. A. Russell, "Fundamental Structural-Acoustic Idealizations for Structures with Fuzzy Internals", Journal of Vibration and Acoustics, **117**, 339–348 (1995).

[30] M. Strasberg and D. Feit, "Vibration damping of large structures induced by attached small resonant structures", J. Acoust. Soc. Am., **99**, 335–344 (1996).

[31] G. Maidanik and J. Dickey, "Design criteria for the damping effectiveness of structural fuzzies", J. Acoust. Soc. Am., **100**, 2029–2033 (1996).

[32] R. L. Weaver, "The effect of an undamped finite degree of freedom "fuzzy" substructure: Numerical Solution and theorical discussion", J. Acoust. Soc. Am., **100**, 3159-3164 (1996).

[33] R. L. Weaver, "Mean and mean-square responses of a prototypical master/fuzzy structure", J. Acoust. Soc. Am., **101**, 1441-1449 (1997).

[34] R. L. Weaver, "Multiple-scattering theory for mean responses in a plate with sprung masses", J. Acoust. Soc. Am., **101**, 3466-3474 (1997).

[35] R. L. Weaver, "Mean-square responses in a plate with sprung masses, energy flow and diffusion", J. Acoust. Soc. Am., **103**, 414-427 (1998).

[36] J.-M. Mencik and A. Berry, "A theoretical formulation of the dynamical response of a master structure coupled with elastic continuous fuzzy subsystems with discrete attachments ", J. Sound Vib., **280**, 1031–1050 (2005).

[37] C. Soize, "A nonparametric model of random uncertainties for reduced matrix models in structural dynamics", Probab. Eng. Mech., **15**, 277–294 (2000).

[38] C. Soize, "Maximum entropy approach for modeling random uncertainties in transient elastodynamics", J. Acoust. Soc. Am., **109**, 1979-1996 (2001).

[39] C. Soize, "A comprehensive overview of a non-parametric probabilistic approach of model uncertainties for predictive models in structural dynamics", J. Sound Vib., **288**, 623–652 (2005).

[40] C. Soize, "Random matrix theory for modeling uncertainties in computational mechanics", Comput. Methods Appl. Mech. Engrg., **194**, 1333–1366 (2005).

[41] J.-F. Durand, "Modélisation de Véhicules en Vibroacoustique Numérique avec Incerti-

tudes de Modélisation et Validation Expérimentale ", "Uncertain computational vibroacoustics modeling of vehicles including model uncertainties and experimental validation", Doctoral thesis, Université de Marne-la-Vallée, France (2007).

[42] J.-F. Durand, C. Soize and L. Gagliardini, "Structural-acoustic modeling of automotive vehicles in presence of uncertainties and experimental identification and validation", *J. Acoust. Soc. Am.*, **124**(3) (2008).

[43] R. Serfling, *Approximations Theorems of Mathematical Statistics* (John Wiley and Sons, New York, 1980).

[44] O.C. Zienkewicz and R.L. Taylor, *The Finite Element Method* (Mac Graw-Hill, New York, 1989). (Fourth edition).

[45] C. Soize, E. Capiez-Lernout, J.-F. Durand, C. Fernandez and L. Gagliardini, "Probabilistic model identification of uncertainties in computational models for dynamical systems and experimental validation", accepted for publication in Comput. Methods Appl. Mech. Engrg., in press, doi:10.1016/j.cma.2008.04.007 (2008).

LIST OF FIGURES

LIST OF FIGURES

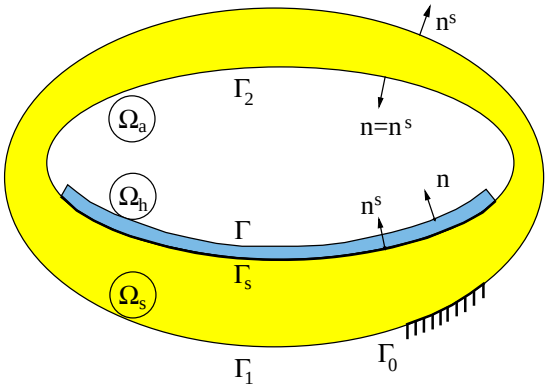

FIG. 1.

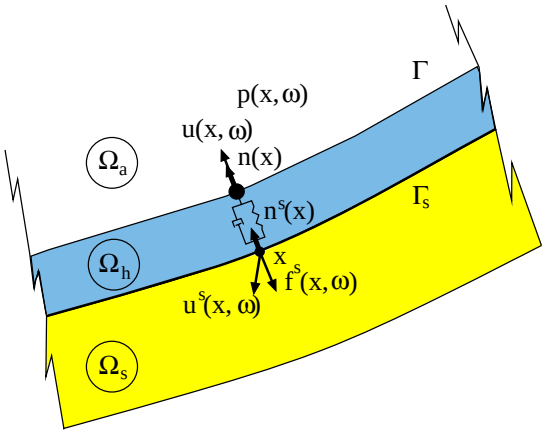

FIG. 2.

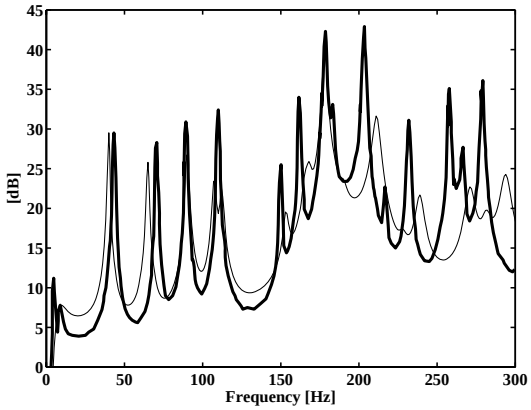

FIG. 3.

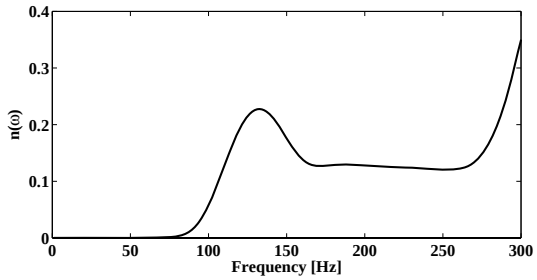

FIG. 4.

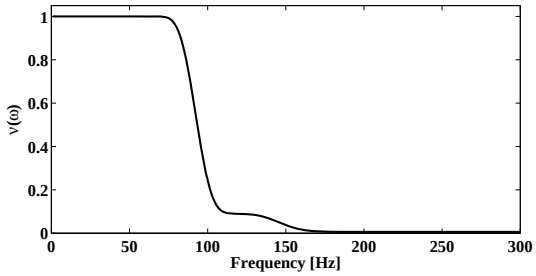

FIG. 5.

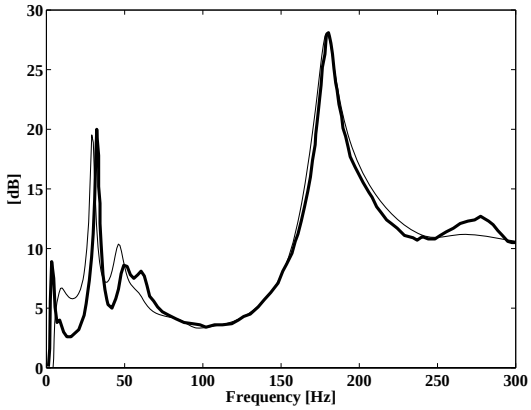

FIG. 6.

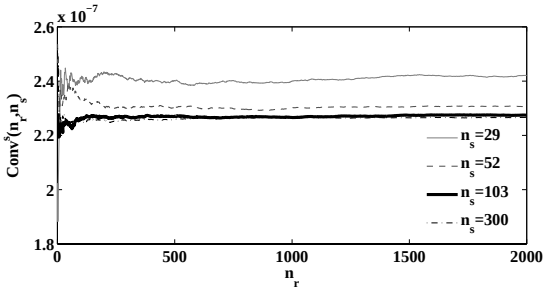
x 10^−7
2.6
2.4
2.2
2
1.8
0
500
1000
1500
2000
n_r
Conv^s(n_r,n_s)
n_s=29
n_s=52
n_s=103
n_s=300

FIG. 7.

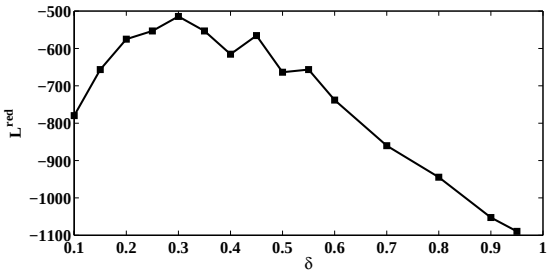

FIG. 8.

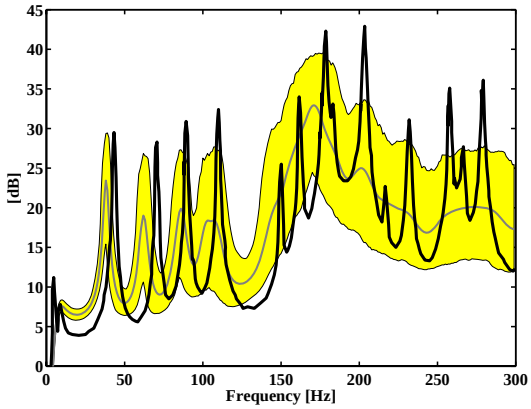

FIG. 9.

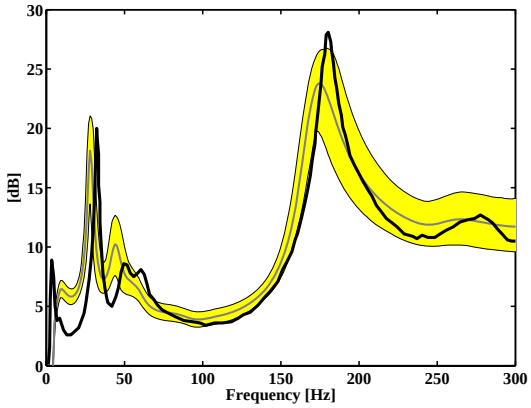

FIG. 10.

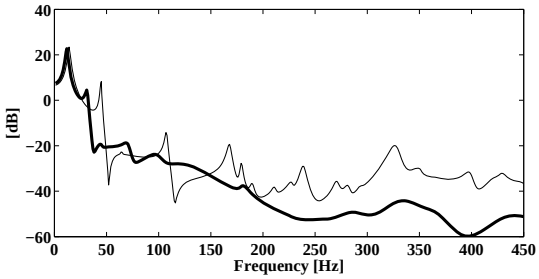
40
20
0
−20
−40
−60
[dB]
0
50
100
150
200
250
300
350
400
450
Frequency [Hz]

FIG. 11.

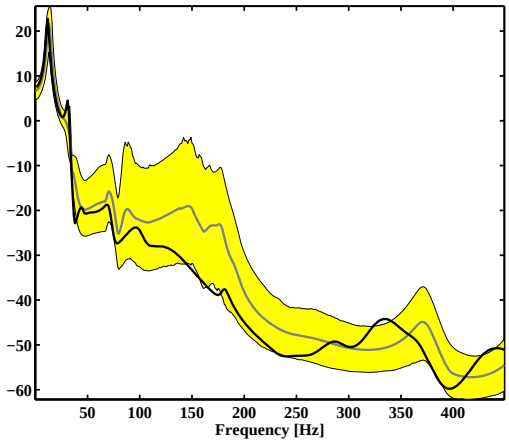
20
10
0
−10
−20
−30
−40
−50
−60
50
100
150
200
250
300
350
400
Frequency [Hz]

FIG. 12.

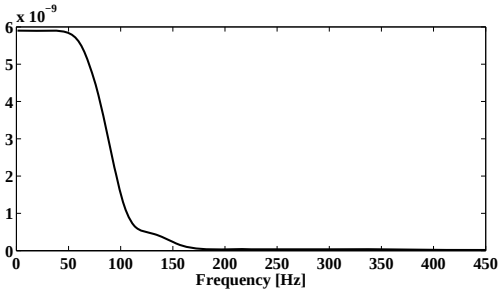

FIG. 13.

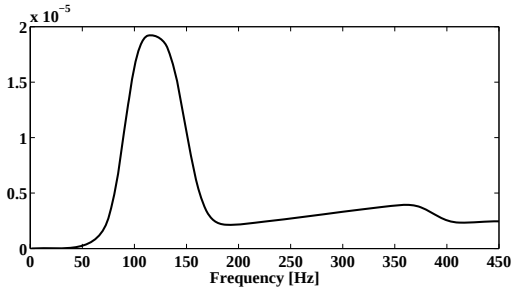

FIG. 14.

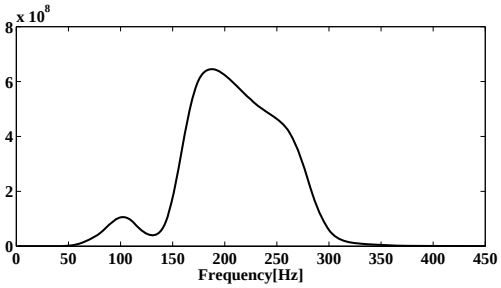

FIG. 15.

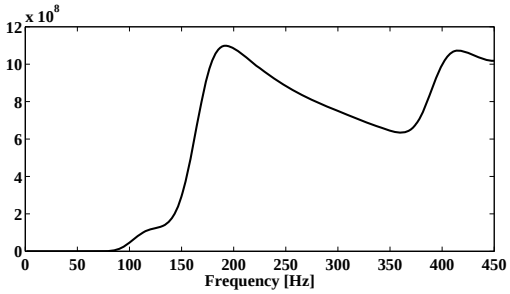
x 10^8
12
10
8
6
4
2
0
0
50
100
150
200
250
300
350
400
450
Frequency [Hz]

FIG. 16.

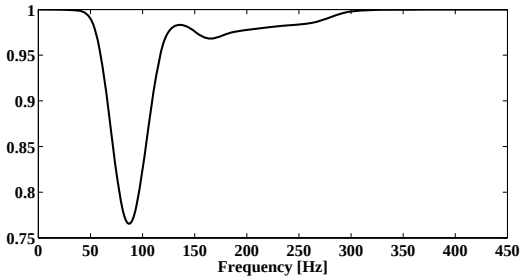
1
0.95
0.9
0.85
0.8
0.75
0
50
100
150
200
250
300
350
400
450
Frequency [Hz]

FIG. 17.

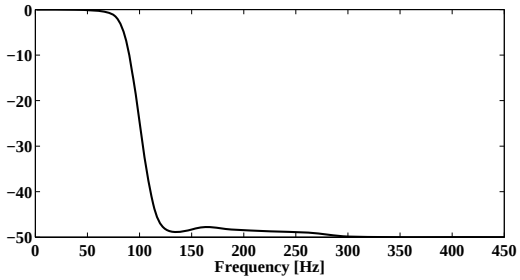

FIG. 18.